Nuclear Physics **A419** (1984) 439–471

INVESTIGATION OF THE ^{47,49}Ti(n, γ)^{48,50}Ti REACTIONS

J.F.A.G. RUYL and J.B.M. DE HAAS

FOM-ECN Nuclear Structure Group, Netherlands Energy Research Foundation, PO Box 1, 1755 ZG Petten, The Netherlands

and

P.M. ENDT and L. ZYBERT*

Fysisch Laboratorium, Rijksuniversiteit Utrecht, The Netherlands

Received 14 October 1983

Abstract: The γ-radiation produced by thermal neutron capture in enriched ^{47}Ti and ^{49}Ti targets has been investigated. In the analysis 57 excited states of ^{48}Ti and 31 of ^{50}Ti have been identified. The Q-value of the ^{47}Ti(n, γ) reaction, 11 626.66(4) keV, is in agreement with previous data. The present value for ^{49}Ti, 10 939.20(4) keV, differs by five standard deviations from a previous result.

The nature of the neutron-capture mechanism has been investigated by comparing the present results with those from previous (d, p) work. It appears that in ^{47}Ti capture proceeds through a doorway state and that the potential capture formalism is valid for ^{49}Ti. Yet the ^{49}Ti cross section for transitions to p-states is predicted low by a factor of 4. The Fermi gas model gives a good representation of the nuclear level density in both nuclei.

The combination of nuclear orientation measurements and circular polarization measurements has yielded the unambiguous determination of the spins of one ^{48}Ti state and of five ^{50}Ti states. Further spin and parity determinations for six ^{48}Ti and for five ^{50}Ti states have been obtained from the analysis of the identified branches together with the results of previous experiments.

Shell-model calculations, which yielded excitation energies, branching ratios, lifetimes and (d, p) spectroscopic factors, give a good representation of the experimental data for the low-lying states in both nuclei.

E NUCLEAR REACTIONS ^{47}Ti(n, γ), (polarized n, $\vec{\gamma}$), ^{49}Ti(n, γ), (polarized n, $\vec{\gamma}$), E = thermal; measured E_γ, $I_\gamma(E_\gamma, \theta)$, γ-CP; deduced Q-values, ^{48}Ti deduced levels, γ-branching, J, π, ^{50}Ti deduced levels, γ-branching, J, π. Enriched, polarized, unpolarized targets.

1. Introduction

This article, in which radiative thermal neutron capture in ^{47}Ti and ^{49}Ti nuclei is treated, is the last in a series of two. In the first article [1]) the ^{48}Ti(n, γ)^{49}Ti reaction has been covered. The latest spectroscopy on the ^{47}Ti(n, γ) and ^{49}Ti(n, γ) reactions has been performed by Fettweis and Saidane [2]) in 1969 and by Tenenbaum *et al.* [3]) in 1971, respectively. Angular-correlation (n, $\gamma\gamma$) measurements of Tenenbaum *et al.* [3,4]) have resulted in spin restrictions for four bound states in ^{48}Ti and for three

* Present address: Department of Physics, University of Birmingham, United Kingdom.

bound states in ^{50}Ti. Further information about spins and parities has been gained by measuring angular distributions in elastic and inelastic scattering experiments [5–7]) and in particle transfer reactions [8–10]). Information about both excitation energies and spins of ^{48}Ti and ^{50}Ti excited states has also been obtained from investigations of the γ-radiation emitted in reactions induced by charged particles [11–13]).

Since the previous measurements experimental techniques have been improved a great deal, thus it was felt that an investigation of the (n, γ) reaction can give a valuable contribution to the knowledge of the decay schemes of both nuclei. Information concerning excitation energies and branching ratios can be obtained from the γ-ray spectra, produced by capture of unpolarized neutrons in unpolarized target nuclei. A measurement of the γ-ray circular polarization resulting from the capture of polarized neutrons and a measurement of the asymmetric γ-ray distribution resulting from the capture of polarized neutrons in polarized target nuclei will provide model-independent information about the spins of excited states. From a survey of all available information final assignments or restrictions on spins and parities will be made.

These results will be used to test shell-model calculations. 1p1h calculations have been performed with the active shells $1f_{7/2}$, $2p_{3/2}$, $1f_{5/2}$ and $2p_{1/2}$.

2. Experiments with unpolarized neutrons

Capture γ-ray spectra were measured at the HFR in Petten with enriched TiO_2 targets (both weighing 8.4 g) at one of the thermal beam facilities. The procedure described in ref. [1]) was used for the experiments and for the calibration of the spectra and thus only some main points will be mentioned here.

Both low-energy (0–2.5 MeV) singles spectra and high-energy (1.8–11.0 MeV) pair spectra were measured with a 30 cm^3 Ge(Li) detector connected to a Tracor Northern 8 k data system. The count rate in the central detector was 3000 s^{-1}, and in the pair mode the triple coincidence count rate was 7 s^{-1} for a timing resolution of 10 ns. In the low-energy spectra the FWHM increased linearly from 1.6 keV at 60 keV to 2.6 keV at 1.3 MeV, in the high-energy spectra from 2.7 keV at 2.2 MeV to 5.4 keV at 6.8 MeV.

The pair spectra were calibrated against the capture γ-rays of ^{2}H and ^{15}N and the singles spectra against the γ-rays emitted by radioactive sources. The ^{2}H γ-ray energy from ref. [14]) was used together with the ^{15}N γ-ray energies from ref. [15]), after correction for the 0.9 ppm higher value of the ^{15}N neutron binding energy reported in ref. [14]). For the γ-rays originating from radioactive sources the energies from ref. [16]) and the intensities from ref. [17]) were taken. As the ^{47}Ti and ^{49}Ti cross sections were known with relatively large errors [18]) (12% and 14%, respectively), absolute intensities were determined by postulating the total ground-state strength to be 100%. This allows for a more accurate determination of the cross sections.

The targets, consisting of TiO_2 powder, were encapsulated in thin-walled teflon cylinders. In the low-energy measurements used for calibration purposes the radioactive sources were placed between detector and target and in the high-energy measurements the target cylinder was surrounded by a second concentric cylinder filled with melamine ($C_3N_6H_6$). These geometries were chosen in order to reduce as much as possible systematic errors originating from irradiation of the detector under different angles.

The abundances and cross sections of the stable Ti isotopes in both target materials are presented in table 1. All five stable Ti isotopes will contribute to the (n, γ) reaction. The present measurements in combination with a separate measurement with a natural Ti target [1]) provided the isotopic assignments of the observed lines.

Background conditions were determined by measuring spectra with a graphite scatterer at the target position.

The singles measurements lasted about 60 h and the pair spectra about 200 h. The calibration measurements took 20 h and 60 h, respectively.

TABLE 1

Abundances and cross sections of the five stable Ti isotopes present in the targets

Isotope	Abundance (%)		σ (b)
	^{47}Ti target	^{49}Ti target	
^{46}Ti	1.9 (1)	2.5	0.59 (18) [a])
^{47}Ti	79.5 (2)	2.3	1.48 (9) [b])
^{48}Ti	16.5 (2)	25.1	7.84 (25) [a])
^{49}Ti	1.1 (1)	67.6	1.67 (12) [b])
^{50}Ti	1.0 (1)	2.5	0.179 (3) [a])

[a]) Ref. [24]).
[b]) From present work.

3. Transitions

In tables 2 and 3 lists of all identified ^{48}Ti and ^{50}Ti transitions are presented. Only statistical errors are given. The systematic error in the γ-ray energies is taken equal to the 2.6 ppm error in the ^{198}Au standard [19]) for the transitions below $E_\gamma = 1.8$ MeV, and to the 3.2 ppm error in the ^{15}N neutron binding energy [14]) for the remaining transitions. The total systematic error in the intensities is estimated as 5%.

Background lines from thermal neutron capture in ^{1}H, ^{7}Li, ^{10}B, ^{12}C, ^{14}N, ^{19}F, ^{23}Na, ^{27}Al, ^{28}Si, ^{35}Cl, ^{40}Ca, ^{53}Cr, ^{56}Fe, ^{58}Ni, ^{63,65}Cu and ^{70,72,73,74,76}Ge were identified.

In total 219 transitions were identified as belonging to the ^{47}Ti(n, γ)^{48}Ti reaction. Most transitions, assigned in ref. [2]), were included except for some misinterpreted

TABLE 2

γ-rays from the $^{47}Ti(n, \gamma)^{48}Ti$ reaction

$E_\gamma + E_r$ [a] (keV)	E_{xi}	E_{xf} [b]	I_γ [c] (%)	[d]
423.631(9)	3782	3359	2.53(3)	CN A
458.45(16)	4197	3739	0.21(4)	U A
802.88(6)	3224	2421	0.323(16)	U PA
811.205(17)	4035	3224	1.26(3)	U A
834.744(17)	4074	3240	1.22(3)	A
840.67(3)	4457	3617	0.602(18)	U A
928.300(10)	3224	2296	2.26(4)	U NPA
944.114(6)	3240	2296	7.79(15)	U NPA
972.92(3)	4197	3224	0.776(22)	U A
983.528(4)	984	0	95.5(18)	UCNPA
1037.611(25)	3333	2296	0.909(24)	NPA
1063.20(5)	3359	2296	0.71(3)	U PA
1086.52(8)	4457	3371	0.370(21)	U
1092.3(3)	4792	3699	0.105(17)	U
1140.95(10)	4758	3617	0.66(7)	U
1158.7(3)	5356	4197	0.22(4)	U A
1182.58(5)	5640	4457	0.486(19)	U
1195.85(6)	3617	2421	0.74(3)	U A
1221.83(8)	4581	3359	0.316(17)	U A
1233.35(12)	4457	3224	0.196(16)	U
1293.73(6)	4911	3617	0.497(22)	A
1312.115(5)	2296	984	32.4(8)	UCNPA
1437.510(19)	2421	984	22.5(6)	UCNPA
1479.363(17)	4719	3240	1.55(4)	U A
1486.84(3)	3782	2296	1.05(3)	C A
1495.56(21)	4719	3224	0.710(25)	A
1539.66(18)	4911	3371	0.25(3)	U A
1556.60(5)	3852	2296	0.79(3)	PA
1572.44(17)	6365	4792	0.169(16)	U
1614.070(18)	4035	2421	2.85(8)	N A
1620.08(18)	6976	5356	0.36(4)	U
1686.66(9)	4911	3224	0.335(18)	
1700.92(16)	4925	3224	0.200(17)	A
1750.52(4)			0.88(3)	
1790.7(3)	5491	3699	0.15(3)	U
1906.12(9)	5146	3240	0.50(3)	U A
1921.67(22)	5146	3224	0.97(16)	A
1933.9(3)	5158	3224	0.62(14)	A
1967.82(23)	6042	4074	0.83(14)	U A
2013.71(16)	2997	984	0.233(20)	NPA
2036.395(11)	4457	2421	6.33(21)	C A
2085.72(16)	5889	3803	0.91(15)	U
2092.056(18)	4388	2296	2.20(7)	U A
2108.7(3)	6827	4719	0.50(11)	
2161.811(12)	4457	2296	7.5(3)	C A
2240.431(17)	3224	984	7.12(25)	U NPA
2285.47(19)	4581	2296	0.35(3)	A
2371.24(8)	4792	2421	0.90(4)	A
2375.274(17)	3359	984	6.88(25)	UCNPA
2387.313(25)	3371	984	2.74(10)	CNPA
2395.68(11)	5620	3224	0.377(22)	A
2420.97(4)	2421	0	1.22(5)	NPA
2463.42(12)			0.314(20)	
2486.5(5)	4783	2296	0.28(7)	U
2489.8(4)	4911	2421	0.30(7)	U A
2498.51(14)	4794	2296	0.81(7)	U A
2517.69(24)	5889	3371	0.44(6)	U
2553.8(3)	6406	3852	0.35(6)	U
2629.2(3)	4925	2296	0.36(6)	A
2633.28(3)	3617	984	9.3(3)	CNPA
2644.6(4)	4940	2296	0.23(5)	U A
2687.60(11)	6490	3803	0.49(3)	U
2715.89(13)	3699	984	0.85(6)	U NPA
2725.8(5)	5146	2421	0.21(5)	U
2756.6(7)	3739	984	0.38(9)	NPA
2819.17(13)	3803	984	0.74(5)	U
2850.10(12)	5146	2296	0.84(6)	U A
2858.9(3)	7616	4758	0.31(5)	U
2868.68(4)	3852	984	3.29(12)	NPA
2885.2(3)			0.33(5)	
2889.0(4)	6627	3739	0.22(5)	U
2907.8(4)	6241	3333	0.21(4)	U
2941.1(4)	6976	4035	0.42(11)	U
2980.5(3)	6314	3333	0.23(4)	U
3070.5(3)	5491	2421	0.22(4)	U
3090.93(6)	4074	984	1.79(6)	N A
3104.5(4)	6957	3852	0.17(4)	U
3121.5(3)			0.26(4)	
3186.46(22)	7574	4388	0.31(4)	U
3198.55(20)	5620	2421	0.37(4)	A
3239.70(18)			0.37(3)	
3252.5(8)	6490	3240	0.08(3)	U
3344.79(9)	7542	4197	0.87(4)	U
3361.29(20)	7061	3699	0.32(3)	U
3371.09(13)	3371	0	0.52(3)	U PA
3403.96(7)	4388	984	2.58(7)	U N A
3467.49(21)	5889	2421	0.87(12)	A
3474.04(9)	4457	984	4.2(3)	UC A
3483.6(3)	6708	3224	0.21(3)	U
3505.08(21)			0.31(3)	
3548.9(4)			0.17(3)	
3574.0(6)	6797	3224	0.09(3)	U
3591.0(6)			0.14(3)	
3596.90(17)	4581	984	0.41(3)	U N A
3616.9(8)	3617	0	0.10(4)	A
3620.4(3)	7359	3739	0.31(4)	U
3633.53(25)	6055	2421	0.24(3)	U
3699.26(12)	3699	0	0.57(3)	U NPA
3714.5(3)			0.18(3)	
3738.51(24)	3739	0	0.60(6)	NPA
3763.9(3)	7616	3852	0.17(3)	U
3775.0(6)	4758	984	0.13(3)	U
3799.80(12)	4783	984	0.56(3)	
3808.74(7)	4792	984	1.10(4)	U A
3843.4(3)			0.189(24)	
3877.0(3)	7616	3739	0.31(5)	U
3886.7(3)			0.212(23)	
3901.6(7)	6898	2997	0.075(22)	U
3917.0(6)	7616	3699	0.13(3)	U
3956.35(16)	4940	984	0.344(24)	U N A
3974.01(22)			0.244(23)	
4010.51(11)	C	7616	0.58(3)	U
4016.78(9)			0.75(3)	
4052.7(3)	C	7574	0.169(22)	U
4069.66(10)	6365	2296	0.69(3)	
4075.3(5)	4074	0	0.29(7)	U
4085.25(12)	C	7542	0.480(24)	U
4135.04(23)	7359	3224	0.37(4)	U
4184.7(15)	7542	3359	0.032(19)	U
4196.83(13)	4197	0	0.494(25)	U
4204.9(5)	4205	0	0.101(20)	
4267.67(6)	C	7359	1.34(3)	U
4275.06(13)			0.442(24)	
4280.68(21)			0.266(23)	
4302.8(4)	7542	3240	0.120(22)	U
4317.0(5)	7542	3224	0.108(22)	U
4328.0(4)			0.132(21)	
4372.77(15)	5356	984	0.341(21)	U A
4379.9(6)			0.082(19)	
4411.3(3)	6708	2296	0.207(22)	U
4429.3(3)			0.140(19)	
4452.5(4)			0.35(4)	
4455.8(5)			0.18(4)	
4492.8(4)			0.090(17)	
4499.77(10)			0.393(21)	
4517.6(8)			0.043(16)	

TABLE 2 (continued)

$E_\gamma + E_r$ [a] (keV)	E_{xi} (keV)	E_{xf} [b] (keV)	I_γ [c] (%)	[d]		$E_\gamma + E_r$ [a] (keV)	E_{xi} (keV)	E_{xf} [b] (keV)	I_γ [c] (%)	[d]
4527.84(19)			0.185(18)			5738.08(5)	C	5889	1.60(3)	U
4536.2(4)	6957	2421	0.087(17)	U		5803.7(3)			0.152(17)	
4566.5(3)	C	7061	0.29(3)	U		5823.47(17)			0.323(18)	
4631.34(20)			0.274(20)			5844.1(5)	6827	984	0.101(17)	U
4650.1(5)	C	6976	0.106(19)	U		5912.7(10)	6898	984	0.055(17)	U
4656.0(6)	5640	984	0.17(4)	U		5966.4(6)			0.094(18)	
4669.2(7)	C	6957	0.096(23)	U		5986.66(3)	C	5640	2.51(4)	U
4698.1(5)			0.096(18)			6007.13(11)	C	5620	0.91(3)	U
4728.31(21)	C	6898	0.262(20)	U		6039.78(19)			0.315(20)	
4793.8(4)	4794	0	0.119(19)	U		6104.29(21)			0.350(23)	
4800.1(3)	C	6827	0.210(20)	U		6135.92(17)	C	5491	0.364(20)	U
4806.24(22)			0.265(21)			6270.29(20)	C	5356	0.68(6)	U
4830.0(3)	C	6797	0.201(22)	U		6375.2(5)	7359	984	0.19(3)	U
4904.69(17)	5889	984	0.308(20)	U	A	6469.00(15)	C	5158	0.94(5)	U
4912.1(8)	4911	0	0.069(19)	U		6480.86(5)	C	5146	4.08(7)	U
4917.9(3)	C	6708	0.169(19)	U		6635.1(7)			0.111(22)	
4937.9(4)	7359	2421	0.27(5)	U		6686.1(3)	C	4940	0.208(21)	U
4956.3(3)			0.176(19)			6701.68(24)	C	4925	0.345(24)	U
5000.25(14)	C	6627	0.382(20)	U		6716.00(11)	C	4911	0.76(3)	U
5058.87(13)	6042	984	0.435(21)	U		6831.5(3)	C	4794	0.82(14)	U
5065.16(9)			0.824(25)			6834.63(15)	C	4792	1.77(14)	U
5070.5(5)	6055	984	0.126(19)	U	A	6843.25(20)	C	4783	0.353(21)	U
5085.05(8)	C	6542	0.638(21)	U		6907.50(6)	C	4719	1.36(3)	U
5129.5(8)			0.064(17)			7045.88(12)	C	4581	0.490(19)	U
5136.19(8)	C	6490	0.707(22)	U		7169.27(3)	C	4457	17.08(20)	UC
5175.23(16)			0.320(18)			7238.99(4)	C	4388	3.61(5)	U
5220.46(11)	C	6406	0.476(19)	U		7420.2(8)	C	4205	0.11(3)	U
5261.5(3)	C	6365	0.27(3)	U		7429.85(7)	C	4197	0.848(19)	U
5306.26(15)			0.419(22)			7591.45(5)	C	4035	3.32(5)	U
5312.9(3)	C	6314	0.73(12)	U		7774.33(6)	C	3852	1.230(25)	U
5315.6(4)			0.47(12)			7844.21(4)	C	3782	2.48(3)	UC
5372.9(5)			0.085(17)			7886.3(9)	C	3739	0.080(13)	U
5387.66(6)	C	6241	0.11(3)	U		7927.1(4)	C	3699	0.119(14)	U
5457.7(5)			0.107(17)			8009.82(4)	C	3617	5.82(8)	UC
5485.2(5)			0.103(17)			8255.96(14)	C	3371	0.443(18)	UC
5506.7(7)	6490	984	0.16(5)	U		8268.1(3)	C	3359	0.31(4)	UC
5509.85(25)			0.47(6)			8386.93(6)	C	3240	1.216(21)	U
5558.4(3)	6542	984	0.45(4)	U		8402.67(12)	C	3224	0.364(12)	U
5571.8(4)	C	6055	0.167(24)	U		9205.64(6)	C	2421	6.48(9)	UC
5584.19(4)	C	6042	3.68(6)	U		9331.02(13)	C	2296	0.297(10)	U
5640.3(10)	5640	0	0.4(5)		A	10643.19(12)	C	984	1.71(3)	UC
5710.8(5)			0.090(17)							

[a]) The recoil energy is written as E_r; errors are purely statistical; the systematic error is 2.6 ppm for energies below 1800 keV and 3.2 ppm for the remaining transitions.

[b]) The capture state is denoted by C.

[c]) Errors are purely statistical; the systematic error is estimated as 5%.

[d]) Arguments for placement:
U – placement unambiguous within three standard deviations;
C – placement observed in $^{47}Ti(n, \gamma\gamma)^{48}Ti$ experiment [4]);
N – placement observed in $^{48}Ti(n, n'\gamma)^{48}Ti$ experiment [20]);
P – placement observed in $^{48}Ti(p, p'\gamma)^{48}Ti$ experiment [21]);
A – placement observed in $^{45}Sc(\alpha, p\gamma)^{48}Ti$ experiment [11]).

single- and double-escape peaks. The most important difference is that the multiplet near 8.26 MeV was resolved in the present work. It consists of the 8256 and 8268 keV transitions of ^{48}Ti and the 8264 keV transition of ^{50}Ti.

Altogether 124 transitions were assigned to the $^{49}Ti(n, \gamma)^{50}Ti$ reaction, including all assignments of ref. [3]).

TABLE 3

γ-rays from the $^{49}Ti(n, \gamma)^{50}Ti$ reaction

$E_\gamma + E_r$ [a] (keV)	$E_{xi} \rightarrow E_{xf}$ [b] (keV)		I_γ [c] (%)	[d]	$E_\gamma + E_r$ [a] (keV)	$E_{xi} \rightarrow E_{xf}$ [b] (keV)		I_γ [c] (%)	[d]
523.762(10)	3199	2675	2.17(3)	U	3707.5(6)	C	7232	0.6(4)	U
733.70(9)	4881	4147	0.214(17)	U	3724.2(5)	6400	2675	0.13(3)	U
760.32(8)	5947	5186	0.340(25)	U	3826.24(11)	5380	1554	0.56(3)	U
1121.143(6)	2675	1554	59.6(13)	C U T	3833.38(24)			0.25(3)	
1156.66(16)	5947	4790	0.200(24)	U	3846.34(11)	6521	2675	1.07(7)	U
1207.946(11)	5380	4172	2.40(6)		3860.3(3)	C	7079	0.20(3)	U
1242.40(4)	6123	4881	0.71(3)	U	3909.2(4)	C	7029	0.140(24)	U
1273.24(19)			0.24(3)		3994.04(5)	5548	1554	1.07(4)	U
1457.6(3)	6838	5380	0.122(23)	U	4054.93(11)	6730	2675	0.52(3)	U
1472.278(6)	4147	2675	11.4(3)	U T	4090.11(8)	C	6849	0.79(3)	U
1497.078(25)	4172	2675	9.6(3)		4101.50(7)	C	6838	0.84(3)	U
1524.55(4)	6711	5186	0.70(3)	U	4151.0(6)			0.085(22)	
1553.811(6)	1554	0	99(5)	C U T	4209.36(6)	C	6730	1.00(3)	U
1636.48(5)	6123	4487	0.601(24)		4218.38(8)			0.75(3)	
1642.43(12)			0.186(16)		4228.62(3)	C	6711	4.01(7)	U
1681.72(15)	4881	3199	0.84(23)	U	4309.94(20)	4310	0	0.259(23)	U T
1730.8(3)	6521	4790	0.24(6)	U	4402.3(5)	7079	2675	0.14(3)	U
1735.03(5)	4410	2675	0.73(3)	U	4417.76(4)	C	6521	1.84(4)	U
1755.8(3)			0.097(19)		4458.13(6)			1.15(3)	
1773.80(20)			0.139(18)		4486.2(4)	4487	0	0.110(20)	U
1852.9(4)	7232	5380	0.55(17)	U	4539.23(18)	C	6400	0.297(22)	U
2001.5(6)			0.30(12)		4559.35(14)	C	6380	0.54(3)	U
2128.4(5)	6302	4172	0.31(10)	U	4602.73(25)	6157	1554	0.200(21)	U
2201.1(3)			0.71(14)		4637.36(4)	C	6302	1.83(4)	U
2205.774(11)	4881	2675	10.1(3)	C U	4747.97(4)	6302	1554	2.03(4)	U
2215.1(5)			0.43(13)		4782.8(4)	C	6157	0.140(21)	U
2300.49(5)	6711	4410	0.68(3)	U	4789.5(4)	4790	0	0.136(21)	U
2305.13(11)			0.287(20)		4816.04(6)	C	6123	1.07(3)	U
2309.04(4)	3863	1554	0.86(4)	U T	4845.9(3)	6400	1554	0.201(21)	U
2348.4(3)	5548	3199	0.36(7)	U	4869.8(6)			0.098(24)	
2511.178(20)	5186	2675	4.26(16)	C U	4898.07(23)			0.28(3)	
2538.44(10)	6711	4172	1.09(8)	U	4992.688(25)	C	5947	4.49(6)	U
2618.40(7)	4172	1554	19.9(7)	C T	5106.8(5)			0.094(18)	
2658.83(20)	6521	3863	0.50(6)		5133.00(25)	C	5807	0.201(19)	U
2700.7(6)	6849	4147	0.16(5)	U	5149.22(8)			0.732(24)	
2705.00(4)	5380	2675	4.38(17)	U	5156.75(7)	6711	1554	0.852(25)	U
2709.3(4)			0.25(5)		5166.68(13)			0.393(21)	
2719.2(3)	7029	4310	0.37(5)	U	5244.34(10)	C	5695	0.547(22)	U
2755.97(13)	4310	1554	1.32(11)	U T	5256.1(5)			0.095(18)	
2765.51(12)			0.73(6)		5283.69(14)	6838	1554	0.366(21)	U
2810.6(5)			0.15(5)		5391.38(5)	C	5548	1.96(4)	U
2846.6(4)			0.24(5)		5396.3(4)			0.177(24)	
2856.22(4)	4410	1554	2.86(11)	U	5412.8(3)			0.173(19)	
2867.48(21)	6730	3863	0.44(5)	U	5420.21(17)			0.327(21)	
2872.81(10)	5548	2675	1.31(8)	U	5498.52(16)			0.352(21)	
2925.0(5)	6123	3199	0.22(5)	U	5525.8(5)	7079	1554	0.126(24)	U
2933.36(12)	4487	1554	0.66(5)	U	5534.50(12)			0.34(3)	
3019.96(11)	5695	2675	0.80(5)	U	5546.6(4)			0.190(24)	
3131.82(19)	5807	2675	0.39(4)	U	5559.269(24)	C	5380	6.14(8)	C U
3182.0(6)	6380	3199	0.13(4)	U	5605.55(23)			0.246(20)	
3186.83(20)			0.37(4)		5678.1(3)	7232	1554	0.165(20)	U
3236.20(7)	4790	1554	1.20(5)	U	5753.047(24)	C	5186	4.72(6)	C U
3271.52(3)	5947	2675	3.81(10)	U	5906.9(8)			0.077(21)	
3448.5(5)	6123	2675	0.14(3)	U	5929.52(15)	7483	1554	0.426(23)	U
3456.30(7)	C	7483	1.03(4)	U	6058.499(20)	C	4881	10.03(11)	C U
3534.6(5)			0.16(3)		6149.26(14)	C	4790	0.53(3)	U
3545.6(6)			0.11(3)		6452.0(5)	C	4487	0.25(4)	U
3565.1(5)			0.13(3)		6529.18(10)	C	4410	0.92(3)	U
3632.24(5)	5186	1554	1.72(5)	C U	6767.22(5)	C	4172	17.8(3)	C U
3636.4(5)			0.13(3)		6791.91(7)	C	4147	7.58(20)	U
3650.0(5)	6849	3199	0.11(3)	U	8264.24(3)	C	2675	8.57(10)	C U
3688.6(7)			0.09(3)		9385.36(6)	C	1554	5.08(7)	C U

4. Placement of transitions

The decay schemes were constructed with the aid of the Ritz combination principle. All results from previous coincidence experiments [3,4,13,20,21]) were included. For ref. [21]) 12 keV was subtracted from the excitation energies of levels above E_x = 3.5 MeV because of calibration errors. Additional levels were accepted on two grounds. Previously observed levels were accepted if they are populated and/or depopulated by at least two transitions and if at least one of the transitions cannot be placed anywhere else in the decay scheme. Previously unobserved levels were added to the decay scheme if they are excited by a primary transition and if they are populated and/or depopulated by at least two unambiguously placed transitions.

In tables 2 and 3 lists of all (recoil corrected) γ-ray energies are given together with the adopted placements, intensities and arguments for placement. The results of the $^{45}Sc(\alpha, p\gamma)^{48}Ti$ reaction [11]) were not included in the analysis because of the difference in reaction mechanism, which results in different states being excited. Nevertheless, a placement also obtained from the $^{45}Sc(\alpha, p\gamma)^{48}Ti$ reaction was considered as a confirmation.

5. Spectroscopic results and discussion

In the present ^{48}Ti decay scheme, consisting of 57 bound states, in total 175 transitions were placed with a χ^2 value of 1.90. Most assignments of previous (n, γ) work [2]) were included, yet due to the greater precision in the present work some misinterpretations were corrected. Levels observed in ref. [2]) were omitted, if they were not populated and/or depopulated by at least two transitions. With respect to previous work altogether 27 bound states, 22 primary and 102 bound-to-bound transitions were added to the (n, γ) decay scheme. In table 4 the branching ratios are presented, derived from the data of table 2.

In total 88 transitions were placed with a χ^2 value of 2.29 in the present decay scheme of ^{50}Ti, which consists of 31 excited states. All assignments from previous coincidence experiments [3,13]) were found to be correct. Altogether 23 bound states, 20 primary and 52 bound-to-bound transitions were added to the decay scheme with respect to previous (n, γ) work. The bound-state branching ratios of table 5 are obtained from the data of table 3.

Footnotes to Table 3

[a]) The recoil energy is written as E_r; errors are purely statistical; the systematic error is 2.6 ppm for energies below 1800 keV and 3.2 ppm for the remaining transitions.

[b]) The capture state is denoted by C.

[c]) Errors are purely statistical; the systematic error is estimated as 5%.

[d]) Arguments for placement:
C – transitions observed in $^{49}Ti(n, \gamma\gamma)^{50}Ti$ coincidence experiment [3]);
U – placement which is within three standard deviations unambiguous;
T – transitions observed in $^{48}Ti(t, p\gamma)^{50}Ti$ coincidence experiment [13]).

TABLE 4

Spin and parity assignments for ^{48}Ti states; for each state the identified decay branches are given as well

J^π	E_{xi} (keV)	E_{xf} (keV)	Branching (%)	J^π	E_{xi} (keV)	E_{xf} (keV)	Branching (%)
2^+	984	0	100	(2^+-4)	4925	2296	64(5)
4^+	2296	984	100			3224	36(5)
2^+	2421	0	5.14(23)	$(2-4)^+$	4940	984	60(6)
		984	94.86(23)			2296	40(6)
0^+	2997	984	100	$(3,4^+)$	5146	2296	34(3)
3^+	3224	984	73.4(8)			2421	8.2(20)
		2296	23.3(7)			3224	38(4)
		2421	3.33(18)			3240	19.9(17)
$(3,4)^+$	3240	2296	100	$(2,3)$	5158	3224	100
6^+	3333	2296	100	$(1-4^+)$	5356	984	61(5)
3^-	3359	984	90.7(5)			4197	39(5)
		2296	9.3(5)	$(1-4)^+$	5491	2421	59(6)
2^+	3371	0	16.0(10)			3699	41(6)
		984	84.0(10)	2^+	5620	2421	50(3)
2^+	3617	0	1.0(4)			3224	50(3)
		984	91.7(5)	2^+	5640	0	39(28)
		2421	7.2(4)			984	16(8)
$(1,2^+)$	3699	0	40.2(22)			4457	45(20)
		984	59.8(22)	2^+	5889	984	12.1(12)
$(1,2)^+$	3739	0	62(6)			2421	34(4)
		984	38(6)			3371	17.3(24)
(2^+-4)	3782	2296	29.4(7)			3803	36(4)
		3359	70.6(7)	4^+	6042	984	34(4)
(0^+-4^+)	3803	984	100			4074	66(4)
3^-	3852	984	80.6(8)	3^-	6055	984	34(4)
		2296	19.4(8)			2421	66(4)
2^+	4035	2421	69.4(8)	4^+	6241	3333	100
		3224	30.6(8)	4^+	6314	3333	100
2^+	4074	0	8.6(20)	3^-	6365	2296	80.1(16)
		984	54.3(15)			4792	19.9(16)
		3240	37.1(12)	(1^--4)	6406	3852	100
$(1,2)^+$	4197	0	33.3(15)	$(1-4)^+$	6490	984	22(6)
		3224	52.4(17)			3240	11(4)
		3739	14.3(22)			3803	67(6)
$(1,2^+)$	4205	0	100	$(1-4^+)$	6542	984	100
4^+	4388	984	54.0(11)	$(1-4)^+$	6627	3739	100
		2296	46.0(11)	4^+	6708	2296	50(5)
3^+	4457	984	22.0(13)			3224	50(5)
		2296	39.0(11)	4^+	6797	3224	100
		2421	33.0(10)	3^-	6827	984	17(4)
		3224	1.02(9)			4719	83(4)
		3371	1.93(12)	$(1,2^+)$	6898	984	42(11)
		3617	3.13(12)			2997	58(11)
3^-	4581	984	38.3(22)	3^-	6957	2421	33(6)
		2296	32.4(24)			3852	67(6)
		3359	29.3(17)	$(1-4)$	6976	4035	54(7)
$(1-4)^+$	4719	3224	31.4(10)			5356	46(7)
		3240	68.6(10)	$(1-4^+)$	7061	3699	100
(0^+-4^+)	4758	984	17(4)	$(1-4)^+$	7359	984	16.8(25)
		3617	83(4)			2421	24(3)
(2^+-4^+)	4783	984	67(6)			3224	33(3)
		2296	33(6)			3739	27(3)
(1^+-4^+)	4792	984	52.3(14)	$(2-4^+)$	7542	3224	9.6(18)
		2421	42.7(14)			3240	10.6(18)
		3699	5.0(8)			3359	2.8(17)
2^+	4794	0	12.8(20)			4197	77(3)
		2296	87.2(20)	(2^+-4)	7574	4388	100
$(1,2)^+$	4911	0	4.8(13)	(1^--4^+)	7616	3699	14(3)
		2421	20(4)			3739	34(4)
		3224	23.2(16)			3852	19(3)
		3371	17.0(18)			4758	34(4)
		3617	34.5(21)				

TABLE 5

Spin and parity assignments for ^{50}Ti states; for each state the identified decay branches are given as well

J^π	$E_{xi} \rightarrow E_{xf}$ (keV)		Branching (%)	J^π	$E_{xi} \rightarrow E_{xf}$ (keV)		Branching (%)
2^+	1554	0	100	4^+	6123	2675	8.1(17)
4^+	2675	1554	100			3199	13(3)
6^+	3199	2675	100			4487	36.0(17)
(0^+-4^+)	3863	1554	100			4881	42.7(19)
4^+	4147	2675	100	$(2-4)^+$	6156	1554	100
3^+	4172	1554	67.5(10)	$(2-4^+)$	6302	1554	87(4)
		2675	32.5(10)			4172	13(4)
2^+	4310	0	16.4(16)	$(4,5)^+$	6380	3199	100
		1554	83.6(16)	(2^+-4^+)	6400	1554	60(6)
3^-	4410	1554	79.6(9)			2675	40(6)
		2675	20.4(9)	$(3,4)^+$	6521	2675	59(3)
2^+	4487	0	14.2(24)			3863	28(3)
		1554	85.8(24)			4790	13(3)
2^+	4790	0	10.1(15)	4^+	6711	1554	25.7(9)
		1554	89.9(15)			4172	32.8(17)
5^+	4881	2675	90.6(19)			4410	20.5(9)
		3199	7.5(19)			5186	21.0(8)
		4147	1.92(17)	$(3-5)^-$	6730	2675	54(3)
$(3,4)^+$	5186	1554	28.8(10)			3863	46(3)
		2675	71.2(10)	$(2-4)^+$	6838	1554	75(4)
4^+	5380	1554	7.6(4)			5380	25(4)
		2675	59.7(11)	$(4^+,5)$	6849	3199	40(10)
		4172	32.7(9)			4147	60(10)
4^+	5548	1554	39.0(17)	$(2-4)^+$	7029	4310	100
		2675	47.7(20)	3^-	7079	1554	48(7)
		3199	13.2(24)			2675	52(7)
(2^+-5)	5695	2675	100	$(2-4)^+$	7232	1554	23(6)
$(2-5)^+$	5807	2675	100			5380	77(6)
$(3,4)^+$	5947	2675	87.6(8)	$(2-4)^+$	7483	1554	100
		4790	4.6(5)				
		5186	7.8(6)				

In tables 6 and 7 the levels identified in the present work are compared to those identified in other experiments. It is shown that in both nuclei at relatively low excitation energy ($E_x < 4$ MeV) only one level is missing in the present work. At higher excitation energy this number increases rapidly. This fact is demonstrated most clearly in ^{48}Ti by the results of the $^{45}Sc(\alpha, p\gamma)$ reaction [11]), where below 7.7 MeV 212 levels have been identified, which is about four times as many as in the present work. Many of these missing levels are presumably high-spin states, which cannot be excited in the (n_{th}, γ) reaction because of lack of momentum transfer.

The present values of the excitation energies of some low-lying ^{48}Ti levels are not in agreement with the values reported by Jackson *et al.* [23]) in 1976. The difference can be explained, however, by the fact that the value of the ^{198}Au standard, which was used in both experiments, has been increased in the meantime.

TABLE 6

Comparison of ^{48}Ti excitation energies (in keV) obtained from different reactions

(n, γ) [a]	(n, γ) [b]	(d, p) [c]	(α, pγ) [d]	(n, n′γ) [e]	(p, p′γ) [f]
0	0	0	0	0	0
983.527(5)	983.7(3)	980(12)	983.5(5)	983(3)	983.35(10)
2295.638(8)	2295.6(5)	2292(12)	2295(1)	2295(5)	2295.5(2)
2421.039(12)	2420.9(5)	2416(12)	2421(1)	2421(6)	2420.3(2)
2997.21(22)			2999(1)	2998(7)	2997.4(3)
3223.940(13)	3223.3(6)	3219(12)	3224(1)	3224(7)	3223.5(2)
3239.752(12)	3239.1(6)		3239(1)	3240(7)	3239.7(4)
3333.25(4)	3332.8(13)	3331(12)	3332(1)	3333(8)	3336(9)
3358.814(20)			3359(1)	3360(8)	3358.7(7)
3370.85(3)	3367.2(18)	3367(12)	3373(1)	3372(8)	3370.7(3)
		3509(12)	3508(1)		
3616.81(3)	3618.1(11)	3620(12)	3618(1)	3618(8)	3621(2)
3699.39(10)			3703(2)	3702(8)	3699(7)
3738.56(15)		3741(8)	3741(2)	3741(8)	3738(5)
3782.447(22)	3782.5(17)	3786(8)	3783(1)	3782(9)	
3802.80(11)					
3852.24(4)		3856(8)	3853(1)	3855(9)	3854(6)
4035.133(19)	4035.7(17)	4036(12)	4036(1)	4035(9)	
			4046(1)	4045(9)	
4074.494(25)		4075(12)	4074(2)	4071(9)	
				4175(9)	
4196.85(4)	4199.5(17)	4198(12)	4199(2)		
4205.3(6)					
		4312(8)	4312(1)		
		4346(8)	4348(2)		
4387.676(23)	4387.7(8)	4390(12)	4389(2)		
4457.439(13)	4457.6(7)	4457(12)	4458(1)		
4580.69(8)		4581(12)	4583(1)		
4719.119(25)	4718.7(18)	4720(12)	4719(1)		
4757.74(14)					
4783.29(14)					
4792.27(7)			4794(2)		
4794.26(17)	4793.5(17)	4795(12)	4795(2)		
		4861(12)	4861(1)		
4910.58(6)	4913.1(21)	4914(12)	4912(2)		
4924.88(17)			4925(2)		
4940.03(19)		4941(12)	4940(1)		
		5000(12)			
5145.81(5)	5146.3(17)	5151(12)	5147(2)		
5157.70(19)	5158.8(2)		5158(2)		
		5255(12)	5252(1)		
		5303(12)	5300(1)		
5356.22(15)	5357.7(18)		5357(2)		
		5382(12)	5383(2)		
	5404.5(17)				
5490.77(19)	5492.8(22)	5493(12)	5490(3)		
		5520(12)	5522(2)		
		5546(12)	5546(2)		
5619.57(10)	5620.2(17)	5619(12)	5620(1)		
5640.00(4)		5635(12)	5640(5)		
		5763(12)	5762(3)		
	5803.7(19)				
5888.55(6)	5890.2(17)	5888(12)	5892(2)		
		5990(12)	5990(1)		
6042.46(5)	6043.6(17)	6043(12)	6044(2)		
6054.5(3)					
	6117.7(17)	6118(12)	6119(2)		
		6144(12)	6147(4)		
6240.6(4)					
6313.7(3)	6316.4(17)	6313(12)	6316(2)		
6365.15(11)	6362.7(18)	6362(12)	6363(3)		
6406.17(14)	6406.4(18)				
6490.45(10)		6489(12)	6491(5)		
6541.63(11)	6541.1(18)		6544(2)		
6626.52(18)	6628.1(18)	6628(12)			
		6681(12)	6682(4)		

TABLE 6 (continued)

(n, γ) [a]	(n, γ) [b]	(d, p) [c]	(α, pγ) [d]	(n, n'γ) [e]	(p, p'γ) [f]
6707.69(25)			6707(2)		
		6747(12)	6744(1)		
6796.8(4)	6797.0(20)				
6827.1(3)					
6898.3(3)					
6957.1(4)			6955(2)		
6976.31(24)			6975(3)		
7060.51(23)					
7358.98(7)	7358.4(17)				
	7453.4(19)				
7541.58(10)					
7574.09(25)			7571(4)		
7616.14(13)					
	7737.6(17)				
	7786.1(19)				
11626.658(20)	11627.6(13)				

[a]) Present work. The errors are purely statistical; a 3.2 ppm systematic error should be added in quadrature.

[b]) Ref. [2]).

[c]) Refs. [8,22]). Energies decreased by 3‰ to correct for calibration differences. Only levels below $E_x = 7.0$ MeV are listed.

[d]) Ref. [11]). Only the relevant levels are listed.

[e]) Ref. [20]). Only levels below $E_x = 4.2$ MeV are listed.

[f]) Ref. [12]) for E_x below 3.5 MeV and ref. [21]) for E_x above 3.5 MeV. From the latter values 12 keV was subtracted to correct for systematic difference.

TABLE 7

Comparison of ^{50}Ti excitation energies (in keV) obtained through different reactions

(n, γ) [a]	(d, p) [b]†	(t, p) [c]†	(p, p') [d]†
0	0	0	0
1553.811(9)	1550(6)	1553.9(12)	1546(15)
2674.955(13)	2678(6)	2675.2(19)	2679(15)
3198.718(20)	3198(20)		3200(15)
	3763(6)	3759(15)	3760(15)
3862.82(6)	3867(20)	3866.2(23)	3870(15)
4147.232(16)	4146(8)	4146(6)	4147(15)
4172.02(3)	4172(8)	4175(4)	4173(15)
4309.87(16)	4313(8)	4307(3)	4311(15)
4410.04(4)	4406(6)	4411(15)	4409(15)
4486.75(8)			
	4522(20)		
	4562(20)		
			4726(15)
4790.00(9)	4794(6)	4784(15)	4795(15)
4880.727(19)	4883(6)	4896(15)	4885(15)
			4976(15)
	5096(8)	5110(15)	
5186.124(25)	5187(6)	5182(15)	5192(15)
	5335(8)		5328(15)
5379.96(3)	5379(6)	5379(15)	5380(15)
	5424(6)	5431(15)	5440(15)
5547.82(5)	5544(6)		
	5583(6)		
		5616(15)	
5694.89(11)	5700(6)	5680(15)	
5806.57(23)	5804(20)		
	5833(20)		

TABLE 7 (continued)

(n, γ) [a]	(d, p) [b]†	(t, p) [c]†	(p, p') [d]†
5946.50(3)	5938(6)		
		6027(15)	
	6061(20)	6050(15)	
6123.18(5)	6120(6)		
6156.5(3)	6157(20)		
	6191(20)	6188(15)	
	6231(6)		
6301.81(4)	6306(20)		
6379.90(21)	6373(6)		
6399.84(21)			
	6479(6)	6472(15)	
6521.42(6)	6516(6)	6528(15)	
	6572(20)		
	6616(6)	6604(15)	
	6677(20)		
6710.59(3)	6706(6)	6704(15)	
6729.88(8)	6724(20)	6736(15)	
6837.65(10)	6842(6)		
6849.07(12)			
	6892(20)		
		6924(15)	
	6965(20)	6971(15)	
	7004(20)		
7029.4(3)	7028(20)	7020(15)	
7078.7(3)	7073(20)	7070(15)	
	7111(20)		
	7156(20)		
	7207(20)	7208(15)	
7232.2(4)	7227(6)		
	7258(20)		
	7365(6)	7365(15)	
	7385(20)		
	7425(20)	7416(15)	
	7449(20)		
7482.98(10)	7481(20)	7472(15)	
	7527(20)		
		7556(15)	
	7608(20)		
	7640(20)	7647(15)	
		7678(15)	

[a]) Present work. The errors are purely statistical; a 3.2 ppm systematic error should be added in quadrature.
[b]) Refs. [8,22]). [c]) Refs. [10,13]). [d]) Ref. [6]).
† Energies decreased by 3‰ to correct for different calibration standard.

The total error in the ^{48}Ti neutron binding energy is 42 eV, consisting of a 20 eV statistical error and a 37 eV systematic error from calibration standards [14,16]). The most recent value of the neutron binding energy has been reported in ref. [24]) as 11 626.5 ± 0.04 keV (where they fail to present the last digit). After an adjustment to 11 626.5(1) keV it is in agreement with the present value of 11 626.66(4) keV.

For ^{50}Ti the 21 eV statistical error and the 35 eV systematic error yield a total error of 41 eV. The present value of the neutron binding energy of 10 939.20(4) keV deviates from the value of 10 939.7(1) keV reported in ref. [24]). A possible explanation for this difference of five standard deviations can be found in the fact that in ref. [24]) only two cascades were used. The chance of systematic errors occurring is

thus larger than for ^{48}Ti and ^{49}Ti, where three and four cascades were used, respectively, and where the agreement with the present values is excellent. The latter were derived from χ^2 procedures in which all placed γ-rays were incorporated.

Taking into account only statistical errors the total observed strength in the ^{47}Ti(n, γ) reaction is equal to $\sum I_\gamma E_\gamma = 86.8(4)$ Q, whereas for the placed transitions one finds $\sum I_\gamma E_\gamma = 82.4(4)$ Q. In the ^{49}Ti(n, γ) reaction we could place a strength of $\sum I_\gamma E_\gamma = 89.4(6)$ Q out of a total observed strength of $\sum I_\gamma E_\gamma = 93.2(6)$ Q. In fig. 1 plots of the intensity flux of all placed transitions are presented. The intensity flux is defined as the total intensity passing through an imaginary level at energy E, and can be obtained from the data given in columns 5 and 6 of tables 8 and 9. From fig. 1 it can be seen that a large part of the primary strength is missing and that, with some fluctuations, the strength increases to 100%, which was assumed for the ground-state feeding. This tendency, which has also been observed in (n, γ)

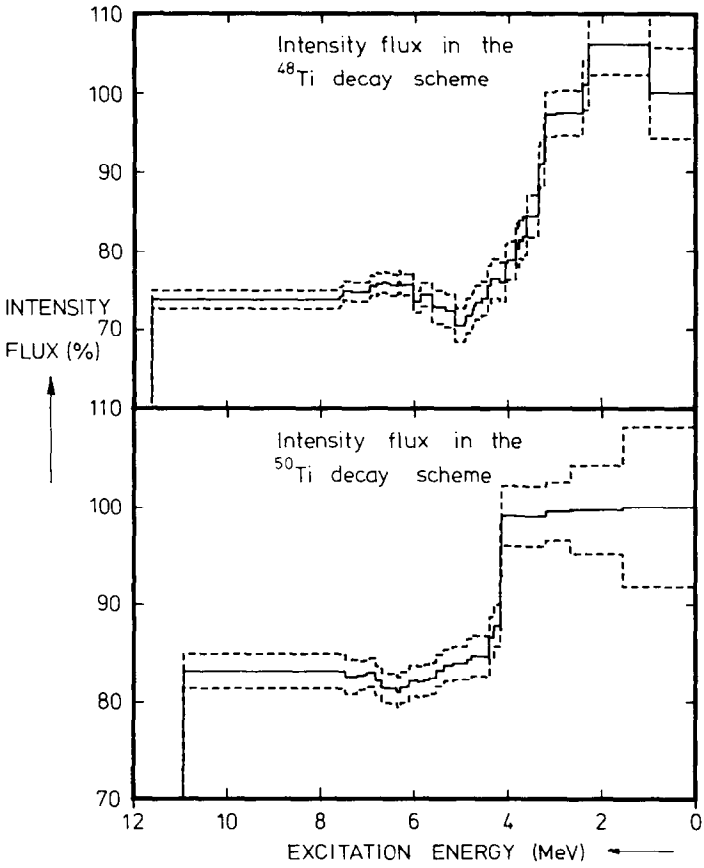

Fig. 1. Intensity flux in the decay schemes of ^{48}Ti (upper part) and of ^{50}Ti (lower part). The dashed curves represent the 99.9% confidence limit. Only statistical errors are taken into account.

experiments with the other even–even final nuclei ^{44}Ca [ref. [25])] and ^{62}Ni [ref. [26])], is a result of the fact that the primary transitions to most levels with $E_x > 5$ MeV are so weak that they cannot be resolved. According to the rules described in sect. 4, these levels will thus not be identified.

TABLE 8

Excitation energies in ^{48}Ti from the present work as compared to those from the (d, p) work; the intensity balance at each level and primary (n, γ) intensities are also given

E_x (keV)		l_n [b])	$(2J+1)S$ [b])	I_γ(%)		
(n, γ) [a])	(d, p) [b])			in	out	primary
0	0			100.0(19)		
983.527(5)	980(12)	3	1.20	101.7(12)	95.5(18)	1.71(3)
2295.638(8)	2292(12)	3	0.33	27.2(3)	32.4(8)	0.297(10)
2421.039(12)	2416(12)	1	0.13	20.2(3)	23.8(6)	6.48(9)
2997.21(22)				0.075(22)	0.233(20	
3223.940(13)	3219(12)	1	0.27	6.59(23)	9.7(3)	0.364(12)
3239.752(12)				4.69(7)	7.79(15)	1.216(21)
3333.25(4)	3331(12)	3	0.58	0.44(6)	0.909(24	
3358.814(20)				3.18(6)	7.59(25)	0.31(4)
3370.85(3)	3367(12)	1+3	0.06+0.04	1.50(7)	3.27(11)	0.443(18)
	3509(12)	(1+)3				
3616.81(3)	3620(12)	1	0.10	7.59(11)	10.2(3)	5.82(8)
3699.39(10)				0.82(6)	1.43(7)	0.119(14)
3738.56(15)	3741(8)	1+3	0.02+0.34	1.13(9)	0.98(11)	0.080(13)
3782.447(22)	3786(8)			2.48(3)	3.58(5)	2.48(3)
3802.80(11)				1.40(16)	0.74(5)	
3852.24(4)	3856(8)			1.92(8)	4.08(12)	1.230(25)
4035.133(19)	4036(12)	1	0.08	3.74(12)	4.11(9)	3.32(5)
4074.494(25)	4075(12)	1	0.04	0.83(14)	3.30(10)	
4196.85(4)	4198(12)			1.93(6)	1.48(5)	0.848(19)
4205.3(6)				0.11(3)	0.101(20	0.11(3)
	4312(8)					
	4346(8)					
4387.676(23)	4390(12)	1	0.31	3.92(6)	4.79(10)	3.61(5)
4457.439(13)	4457(12)	1	0.26	17.56(20)	19.2(5)	17.08(20)
4580.69(8)	4581(12)			0.490(19)	1.08(5)	0.490(19)
4719.119(25)	4720(12)	1	0.14	1.85(11)	2.26(5)	1.36(3)
4757.74(14)				0.31(5)	0.80(8)	
4783.29(14)				0.353(21)	0.84(7)	0.353(21)
4792.27(7)				1.94(14)	2.11(6)	1.77(14)
4794.26(17)	4795(12)	1	0.06	0.82(14)	0.93(7)	0.82(14)
	4861(12)	1	0.11			
4910.58(6)	4914(12)	1	0.09	0.76(3)	1.44(8)	0.76(3)
4924.88(17)				0.345(24)	0.56(7)	0.345(24)
4940.03(19)	4941(12)	1	0.06	0.208(21)	0.57(6)	0.208(21)
	5000(12)					
5145.81(5)	5151(12)	1	0.26	4.08(7)	2.51(18)	4.08(7)
5157.70(19)				0.94(5)	0.62(14)	0.94(5)
	5255(12)					
	5303(12)					
5356.22(15)				1.04(7)	0.56(5)	0.68(6)
	5382(12)	1+3	0.03+0.18			
5490.77(19)	5493(12)	1+3	0.01+0.08	0.364(20)	0.37(5)	0.364(20)
	5520(12)					
	5546(12)					
5619.57(10)	5619(12)	1	0.11	0.91(3)	0.75(4)	0.91(3)
5640.00(4)	5635(12)	1	0.44	2.51(4)	1.1(5)	2.51(4)
	5763(12)					
5888.55(6)	5888(12)	1	0.17	1.60(3)	2.53(20)	1.60(3)
	5990(12)	1+3	0.02+0.10			
6042.46(5)	6043(12)	1	0.22	3.68(6)	1.26(14)	3.68(6)
6054.5(3)				0.167(24)	0.37(3)	0.167(24)
	6118(12)					
	6144(12)	1	0.02			
6240.6(4)				0.11(3)	0.21(4)	0.11(3)
6313.7(3)	6313(12)	1	0.20	0.73(12)	0.23(4)	0.73(12)
6365.15(11)	6362(12)	1	0.08	0.27(3)	0.85(3)	0.27(3)
6406.17(14)				0.476(19)	0.35(6)	0.476(19)
6490.45(10)	6489(12)	1+3	0.04+0.42	0.707(22)	0.72(7)	0.707(22)
6541.63(11)				0.638(21)	0.45(4)	0.638(21)

TABLE 8 (continued)

E_x (keV)		l_n [b]	$(2J+1)S$ [b]	I_γ (%)		
(n, γ) [a]	(d, p) [b]			in	out	primary
6626.52(18)	6628(12)			0.382(20)	0.22(5)	0.382(20)
	6681(12)	1+3	0.11+0.46			
6707.69(25)				0.169(19)	0.42(4)	0.169(19)
	6747(12)	1+3	0.11+0.07			
6796.8(4)				0.201(22)	0.09(3)	0.201(22)
6827.1(3)				0.210(20)	0.60(11)	0.210(20)
6898.3(3)				0.262(20)	0.13(3)	0.262(20)
6957.1(4)				0.096(23)	0.26(4)	0.096(23)
6976.31(24)				0.106(19)	0.78(12)	0.106(19)
7060.51(23)				0.29(3)	0.32(3)	0.29(3)
7358.98(7)				1.34(3)	1.14(8)	1.34(3)
7541.58(10)				0.480(24)	1.13(5)	0.480(24)
7574.09(25)				0.169(22)	0.31(4)	0.169(22)
7616.14(13)				0.58(3)	0.91(8)	0.58(3)
11626.658(20)					73.8(4)	

[a]) Present work. The errors are purely statistical; a 3.2 ppm systematic error should be added in quadrature.

[b]) Refs. [8,22]). The energies are decreased by 3‰ to correct for calibration difference.

Postulating a 100% feeding of the ground state it is possible to determine the ^{47}Ti and ^{49}Ti (n, γ) cross sections σ_γ with respect to the (n, γ) cross section of ^{48}Ti [ref. [18])]. This way we find $\sigma_\gamma = 1.48(9)$ b for ^{47}Ti and $\sigma_\gamma = 1.67(12)$ b for ^{49}Ti. The error consists mainly of two parts: the error in the ^{48}Ti cross section (4%) and the probability of missed intensity to the ground state, which was estimated as 5%.

6. Experiments with polarized neutrons

Spins of several levels were assigned by means of the measured angular distribution of strong primary γ-rays resulting from capture of polarized neutrons in polarized target nuclei. For this purpose the measured γ-ray circular polarization resulting from capture of polarized neutrons in unoriented target nuclei was utilized as well. In the next two subsections the experiments will be described.

6.1. THE NUCLEAR ORIENTATION EXPERIMENT

To polarize the target nuclei the "brute force" method was employed, where the target, cooled down to extremely low temperatures (±10 mK), is placed in a high magnetic field (7.5 T). For this purpose the two TiO_2 targets (see sect. 1) had to be reduced to metallic Ti in order to improve the heat conductivity. This was done with CaH_2 as a reducing agent at 900°C in a molybdenum crucible under vacuum conditions. The reaction

$$2CaH_2 + TiO_2 \rightarrow 2CaO + Ti + 2H_2 \qquad (1)$$

is described in more detail in ref. [27]). The ingots were prepared by means of an arc-melt of the Ti powder in a carbon crucible. This is the most critical step in the process as the powder is highly inflammable under normal conditions. The reaction yields were about 94% and 50% for ^{47}Ti and ^{49}Ti, respectively. The ^{47}Ti ingot was clamped tightly in an Al target holder. For the ^{49}Ti sample as well the Ti metal and the Al target holder were electroplated with pure tin and subsequently tin-soldered to each other. With the latter method a better heat conductivity between target and Al target holder was achieved than by clamping them together.

The target was cooled by means of a nuclear demagnetization stage (coolant material $PrNi_5$), which was precooled to 25 mK in a 6 T magnetic field by a ^{3}He–^{4}He dilution refrigerator. After closing the heat switch between the refrigerator and the nuclear stage the field was reduced, resulting in a lowering of the temperature. An average temperature of about 10 mK could be achieved for periods up to two weeks. The target temperature was monitored by means of a Co thermometer, mounted under the Al target holder. This Co thermometer consists of a single crystal of hcp Co which was irradiated by neutrons to form ^{60}Co nuclei in the lattice. As hcp Co is a ferromagnet, a well-defined hyperfine field will be present at the position of

TABLE 9

Excitation energies in ^{50}Ti from the present work as compared to those from the (d, p) work; the intensity balance at each level and primary (n, γ) intensities are also given

E_x (keV)		l_n [b]	$(2J+1)S$ [b]	I_γ(%)		
(n, γ) [a]	(d, p) [b]			in	out	primary
0	0	3	0.76	100(3)		
1553.811(9)	1550(6)	1+3	0.08+0.32	99.2(15)	99(3)	5.08(7)
2674.955(13)	2678(6)	1+3	0.04+0.01	59.4(6)	59.6(13)	8.57(10)
3198.718(20)	3198(20)			1.65(25)	2.17(3)	
	3763(8)					
3862.82(6)	3867(20)			0.94(8)	0.86(4)	
4147.232(16)	4146(8)	1	0.74	7.95(21)	11.4(3)	7.58(20)
4172.02(3)	4172(8)	1	0.93	21.6(4)	29.5(8)	17.8(3)
4309.87(16)	4313(8)	1	0.02	0.37(5)	1.58(11)	
4410.04(4)	4406(8)	0+2	0.003+0.009	1.60(4)	3.59(11)	0.92(3)
4486.75(8)				0.85(5)	0.77(5)	0.25(4)
	4522(20)					
	4562(20)					
4790.00(9)	4794(6)	1	0.05	0.98(7)	1.34(6)	0.53(3)
4880.727(19)	4883(6)	1	0.81	10.75(11)	11.1(4)	10.03(11)
	5096(8)					
5186.124(25)	5187(6)	1	0.20	5.76(7)	5.98(17)	4.72(6)
	5335(8)					
5379.96(3)	5379(6)	1	0.23	6.81(19)	7.34(18)	6.14(8)
	5424(6)	1+3	0.01+0.06			
5547.82(5)	5544(6)	1	0.03	1.96(4)	2.75(11)	1.96(4)
	5583(6)	1+3	0.01+0.08			
5694.89(11)	5700(6)			0.547(22)	0.80(5)	0.547(22)
5806.57(23)	5804(20)	1+3	0.004+0.08	0.201(19)	0.39(4)	0.201(19)
	5833(20)	1+3	0.02+0.13			
5946.50(3)	5938(6)	1	0.29	4.49(6)	4.35(11)	4.49(6)
	6061(20)	1	0.02			
6123.18(5)	6120(6)	1+3	0.15+0.50	1.07(3)	1.67(7)	1.07(3)
6156.5(3)	6157(20)	1	0.02	0.140(21)	0.200(21)	0.140(21)
	6191(20)					
	6231(6)					

TABLE 9 (continued)

E_x (keV)		l_n [b]	$(2J+1)S$ [b]	I_γ(%)		
(n, γ) [a]	(d, p) [b]			in	out	primary
6301.81(4)	6306(20)			1.83(4)	2.34(11)	1.83(4)
6379.90(21)	6373(6)	1	0.07	0.54(3)	0.13(4)	0.54(3)
6399.84(21)				0.297(22)	0.34(4)	0.297(22)
	6479(6)	1	0.04			
6521.42(6)	6516(6)	1+3	0.09+0.47	1.84(4)	1.82(11)	1.84(4)
	6572(20)					
	6616(6)	3	0.26			
	6677(20)					
6710.59(3)	6706(6)	1	0.25	4.01(7)	3.31(9)	4.01(7)
6729.88(8)	6724(20)	0	0.01	1.00(3)	0.96(6)	1.00(3)
6837.65(10)	6842(6)	1+3	0.09+0.41	0.84(3)	0.49(3)	0.84(3)
6849.07(12)				0.79(3)	0.26(6)	0.79(3)
	6892(20)					
	6965(20)					
	7004(20)	1	0.05			
7029.4(3)	7028(20)	1	0.03	0.140(24)	0.37(5)	0.140(24)
7078.7(3)	7073(20)	2	0.03	0.20(3)	0.26(3)	0.20(3)
	7111(20)	2	0.05			
	7156(20)	3	0.17			
	7207(20)	1	0.02			
7232.2(4)	7227(6)	1	0.09	0.6(4)	0.71(17)	0.6(4)
	7253(20)	3	0.01			
	7365(6)	2+4	0.005+0.56			
	7385(20)	1	0.02			
	7425(20)					
	7449(20)	1	0.04			
7482.98(10)	7481(20)	1+3	0.09+0.13	1.03(4)	0.426(23)	1.03(4)
	7527(20)					
	7608(20)	1	0.09			
	7640(20)					
10939.204(21)					83.2(6)	

[a]) Present work. The errors are purely statistical; a 3.2 ppm systematic error should be added in quadrature.

[b]) Refs. [8,22]). The energies are decreased by 3‰ to correct for calibration difference.

the radioactive ^{60}Co nuclei. The γ-radiation emitted by ^{60}Co is of pure E2 character, with a unique dependence of anisotropy on temperature due to the nuclear orientation of the Co.

The neutrons were polarized by means of Bragg reflection from a magnetized Cu_2MnAl Heusler single crystal. The neutron beam, which was diffracted under an angle of 16.3°, consisted mainly of 88 meV neutrons with a degree of polarization of 95%.

An r.f. spin flipper was employed to rotate the neutron spin from parallel (⇈) to antiparallel (⇅) with respect to the target spin orientation. During the measurements the total neutron flux through the target was monitored by means of a fission counter and the neutron polarization by means of an analysing crystal in combination with a BF_3 counter, which were both mounted behind the sample.

Capture γ-ray spectra were measured under angles of 0° and of 90° with respect to the target orientation axis with two Ge(Li) detectors, both having an efficiency of 15%. The FWHM of the 0° and 90° detectors at 7.2 MeV was in the ^{47}Ti

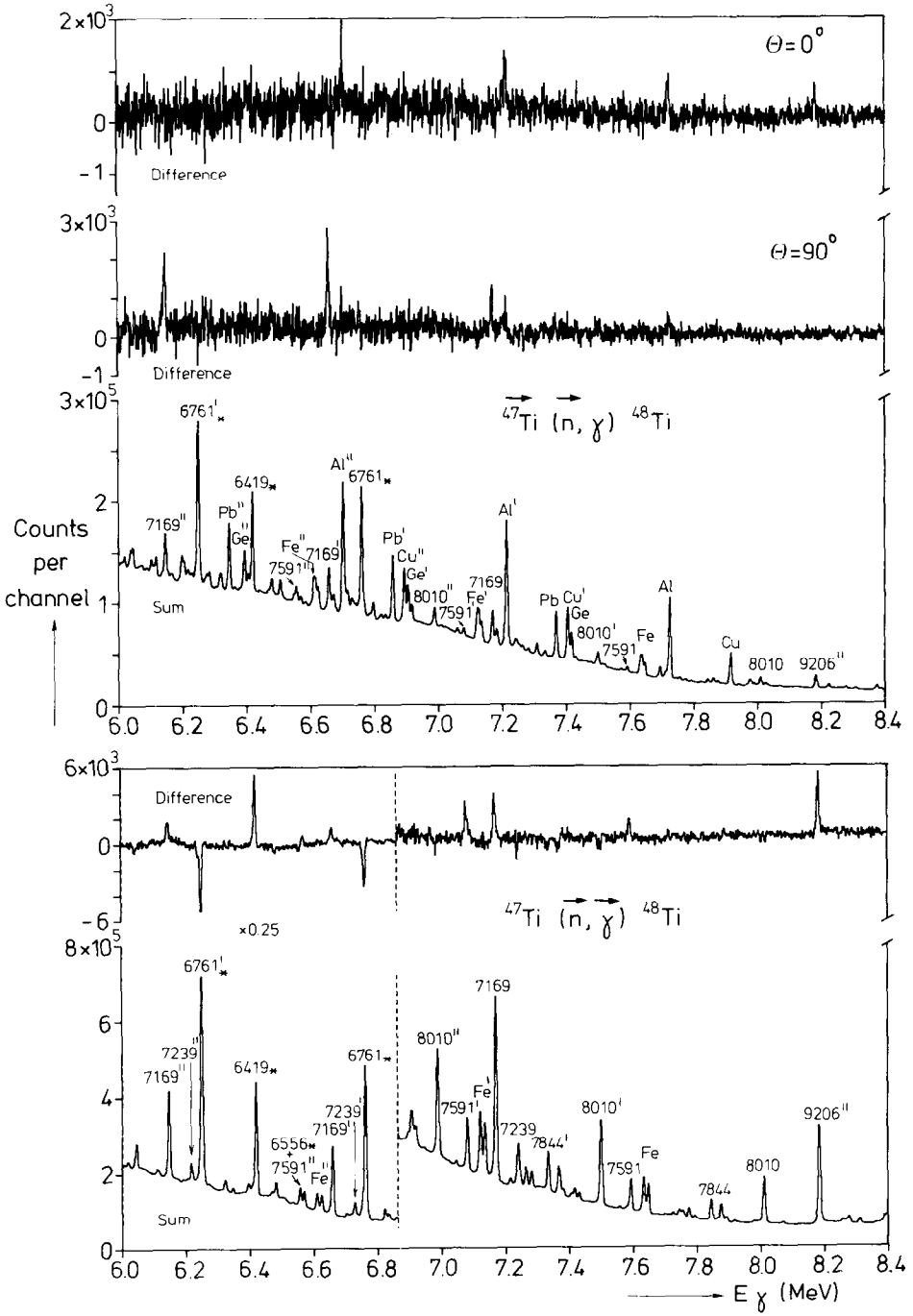

Fig. 2. Part of the spectra for the angular distribution measurement (upper part) and for the circular polarization measurement (lower part) with a ^{47}Ti target. The difference spectra between the modes with neutron spin and target spin parallel and antiparallel for the 0° and 90° detectors are presented for the angular distribution measurement. The sum spectrum of the 90° detector is presented as well. For the circular polarization measurement the sum and difference spectra are also presented but now for opposite neutron orientations. Transitions labelled with an asterisk originate from the ^{48}Ti(n, γ) reaction.

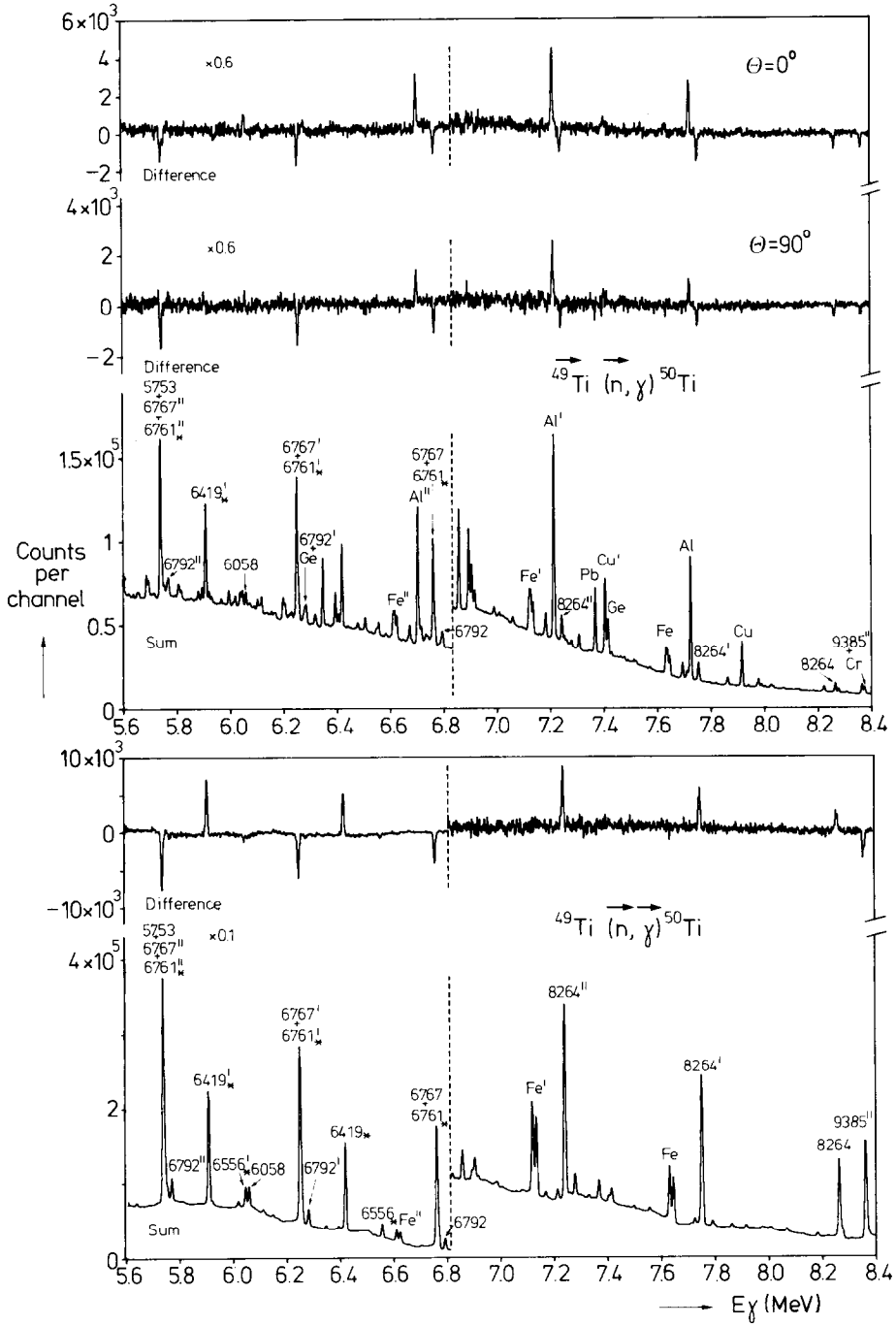

Fig. 3. As fig. 2, but with ^{49}Ti instead of ^{47}Ti.

measurement 9.9 keV and 7.2 keV and in the ^{49}Ti measurement 6.7 keV and 6.2 keV, respectively. The spectra, measured for different neutron orientation, and the data from the beam monitors were stored in different halves of the memory of a 20 k Tracor Northern TN 11 system and dumped on tape every 12 h.

In figs. 2 and 3 parts of the total spectra are presented, resulting from 1000 h of data accumulation with the ^{47}Ti sample and from 1000 h with the ^{49}Ti sample.

6.2. THE CIRCULAR POLARIZATION EXPERIMENT

The circular polarization measurements were performed with the TiO_2 targets as described in ref. [1]). In order to achieve a consistent treatment of the data the circular polarization coefficient, referred to as R in ref. [1]), is called A_1^{10} in the present paper. In figs. 2 and 3 parts of the final spectra, resulting from 1600 h of measuring time with the ^{47}Ti target and from 1200 h with the ^{49}Ti target, are presented in order to give an impression of the achieved statistical accuracy.

7. Method of analysis

An extensive discussion of the data reduction method is given in refs. [28,29]). Some relevant facts will be mentioned here.

In general the angular distribution of capture γ-rays is given by the expression

$$I_\gamma(\theta) = \sum_{k,k_1,k_2} A_k^{k_1 k_2} f_{k_1}(n) f_{k_2}(J_t) P_k(\cos\theta)\,, \tag{2}$$

where f_k are the orientation parameters of the nuclei (or neutrons), P_k are Legendre polynomials and $A_k^{k_1 k_2}$ are spin-dependent coefficients [28]). The integer values of k are restricted to $0 \leq k \leq 2$ for dipole radiation, which will be assumed throughout the rest of this article. The values of k_2 range in principle from 0 to $2J_t$, where J_t is the spin of the target nucleus, but if $f_1(J_t)$ is below 10% the higher-order polarization parameters $f_{k_2}(J_t)$ with $k_2 \geq 2$ can be neglected. Expression (2) then reduces to

$$I_{\gamma_{n.o.}}(\theta) \sim 1 + f_1(n) f_1(J_t)[A_0^{11} + A_2^{11} P_2(\cos\theta)] \tag{3a}$$

for nuclear orientation experiments and to

$$I_{\gamma_{c.p.}}(\theta) \sim 1 + \varepsilon_c[A_1^{10} f_1(n) + A_1^{01} f_1(J_t)] P_1(\cos\theta) \tag{3b}$$

for circular polarization experiments, where ε_c is the efficiency for the detection of circular polarization.

As thermal neutron capture mainly proceeds through s-wave capture two values of the compound spin J_c are possible, $J_c = J_t \pm \frac{1}{2}$. The relative contribution of the higher-spin channel ($J_c = J_t + \frac{1}{2}$) is denoted by the channel spin admixture α_f. Between the two capture channels coherent interference may occur, and thus two different A-values may exist for the same α_f and final spin J_f depending on whether the

interference is constructive or destructive. Only in cases where transitions can arise from only one capture channel the A-coefficients have definite values.

Now one may define the relative asymmetry $e(\theta)$ as

$$e(\theta)=\frac{I(\theta)_{\uparrow\uparrow}-I(\theta)_{\uparrow\downarrow}}{I(\theta)_{\uparrow\uparrow}+I(\theta)_{\uparrow\downarrow}}, \tag{4}$$

where $I(\theta)_{\uparrow\uparrow}[I(\theta)_{\uparrow\downarrow}]$ is $I(\theta)$ with target and neutron spins parallel [antiparallel]. Then the A-coefficients can be extracted from the data of the nuclear orientation experiment using the following expressions:

$$A_0^{11}=\frac{e(0°)+2e(90°)}{3f_1(n)f_1(J_t)}, \tag{5}$$

$$A_2^{11}=\frac{2[e(0°)-e(90°)]}{3f_1(n)f_1(J_t)}. \tag{6}$$

The A_0^{11} coefficient, which is independent of final spin J_f and interference sign, is directly related to α_f by

$$\alpha_f=\frac{J_t+1}{2J_t+1}[A_0^{11}+1]. \tag{7}$$

In the actual circular polarization experiment with polarized neutrons, $f_1(n)\approx 1.0$, and randomly oriented target nuclei, $f_1(J_t)=0$, expression (3b) reduces to

$$I_\gamma(\theta)\sim 1+\varepsilon_c A_1^{10} f_1(n) P_1(\cos\theta). \tag{8}$$

Because the spectra were measured with two opposite neutron orientations ($\theta=0°$ and $\theta=180°$) the value of the A_1^{10} coefficient can be obtained from

$$A_1^{10}=\frac{1}{\varepsilon_c f_1(n)}\frac{[I(0°)-I(180°)]}{[I(0°)+I(180°)]}. \tag{9}$$

The energy dependence of ε_c is well known [29]) and the product $\varepsilon_c f_1(n)$ could be calibrated against the 6419 keV transition in ^{49}Ti, for which the A_1^{10} value is known to be +1.00 [ref. [1])]. The latter transition can be used because there is an appreciable amount of ^{48}Ti present in the targets (see table 1).

With the measured A-values a chi-squared method can be used for all final spin possibilities with α_f as running parameter. A final spin J_f is excluded if for all α_f and for both interference signs the chance of finding this J_f is excluded at a 99.9% confidence limit.

Different methods were used to determine the average target temperatures in the two nuclear orientation measurements. This temperature can be directly derived from $f_1(J_t)$ via the Boltzmann distribution. The temperature indicated by the Co thermometer was not accepted as the temperature of the Ti nuclei because there is some distance between the Co crystal and the sample, which may cause a difference

in temperature. The following methods were used to determine the temperature. In the $^{49}\vec{\text{Ti}}(\vec{n}, \gamma)$ experiment there are strong primary transitions which have no channel interference as they populate levels with spin $J = J_t \pm \frac{3}{2}$. For these transitions ($E_\gamma = 6058$ and 9385 keV) the theoretical values of the A-coefficients are known. In the temperature range indicated by the Co thermometer (5–20 mK) the χ^2 was calculated. The value at the minimum of χ^2 was taken as the value for $f_1(J_t)$ and the standard deviation was determined in the way described in ref. [30]).

In the $^{47}\vec{\text{Ti}}(\vec{n}, \gamma)$ experiment no strong primaries are present populating levels with $J = J_t \pm \frac{3}{2}$. In this case the strongest primary, $E_\gamma = 7169$ keV, exciting the level at $E_x = 4457$ keV, served as a calibration standard. From the data of the Co thermometer we find that the temperature lies between 10 and 20 mK. The chi-squared method shows that $J = 3$ is the only solution in this temperature range that satisfies the 99.9% confidence limit. The value of $f_1(J_t)$ was determined by minimizing χ^2 for $J = 3$ in the two-dimensional area spanned by $T = 10$–20 mK and channel spin admixture $\alpha_f = 0$–1.

8. Spins and parities

8.1. ^{48}Ti

From the nuclear orientation experiment a value of 0.069(5) was obtained for the average target polarization. For the ^{47}Ti target nucleus with a magnetic moment of -0.79 nm and a spin J_t of $\frac{5}{2}$ in a magnetic field of 7.5 T we obtain from this degree of polarization an average temperature of 15(1) mK.

The combined results of the nuclear orientation experiment and of the circular polarization experiment are presented in table 10. It appears that the circular polarization experiment yields a larger number and more precise A-coefficients than the nuclear orientation experiment. This is caused by the fact that the beam intensity is larger by an order of magnitude and that the circular polarization spectra have much less background radiation, as is clearly demonstrated in fig. 2.

For four states the analysis yielded only one solution for the spin. The $J = 2$ assignments for the levels at 2421, 3617 and 4035 keV, based upon momentum transfer measurements in the (α, α') reaction [5]), were confirmed. To the level at 4457 keV an unambiguous spin assignment of $J = 3$ was made. This assignment is reconfirmed by the 2036 and 2162 keV secondary transitions depopulating the level. The respective A-coefficients of these secondaries are in agreement with theoretical values, calculated as described in ref. [31]) for an intermediate $J = 3$ state decaying to $J = 2$ and $J = 4$ levels, respectively. For the remaining 15 investigated levels the present work allows only spin restrictions.

The average fraction $\langle \alpha_f \rangle$ of the high-spin ($J_c = 3$) channel in the neutron-capture process was determined through the primary transitions listed in table 10. For these transitions, with a total strength of 48.6(3)%, the intensity-weighted average value

TABLE 10

Results from analysis of the nuclear orientation and of the circular polarization measurements for ^{48}Ti states

E_x	$E_\gamma + E_r$ (keV)	A_1^{10}	A_0^{11}	A_2^{11}	J
984	10 643	−0.26 (12)	−0.63 (14)	−0.17 (19)	(1–3)
2296	9331	−0.6 (3)	0.4 (3)	0.0 (4)	(2–4)
2421	9206	0.94 (4)	0.33 (6)	0.50 (7)	2
3224	8403	1.2 (4)			(2, 3)
3240	8387	−0.32 (15)	0.9 (4)	−0.7 (6)	(2–4)
3617	8010	−0.15 (4)	0.11 (13)	0.23 (21)	2
3782	7844	−0.35 (9)	0.60 (24)	0.5 (3)	(2–4)
3852	7774	0.03 (21)			(1–4)
4035	7591	1.05 (8)	0.41 (20)	0.6 (3)	2
4197	7430	−0.2 (4)			(1–4)
4388	7239	−0.41 (10)	0.21 (18)	0.01 (24)	(2–4)
4457	7169	0.38 (25)	0.65 (6)	−0.56 (7)	3
	2036		0.76 (8)	0.33 (11)	
	2162		0.69 (8)	−0.12 (11)	
4719	6908	−0.12 (24)			(1–4)
5146	6481	−0.53 (8)	1.0 (3)	0.0 (5)	(3, 4)
5158	6469	0.8 (3)			(2, 3)
5620	6007	−0.7 (4)			(1–4)
5640	5987	−0.57 (18)	−1.0 (5)	0.2 (6)	(1–3)
6042	5584	−0.52 (11)			(2, 3)
7359	4268	1.3 (3)			(2, 3)

of A_0^{11} was 0.50(5), which corresponds to a value of 0.88(3) for $\langle \alpha_f \rangle$. If σ^- and σ^+ are defined as the cross sections for the low- and high-spin channel, respectively, then the transitions of table 10 yield values of 0.086(22) b for σ^- and of 0.63(5) b for σ^+. In a recent compilation [18]) one finds from the known positive-energy resonances a value of 0.07 b for σ^- and of 0.80 b for σ^+. In the latter work only one $J = 2$ negative-energy resonance is listed. The presently investigated 48.6% primary strength exhausts largely the 0.80 b for σ^+ and as there is no reason to assume that the remaining 51.4% primary strength behaves differently and will proceed mainly through the low-spin channel, the present results strongly suggest that there is also a negative-energy $J = 3$ resonance which considerably contributes to the thermal neutron cross section.

8.2. ^{50}Ti

The average target polarization in the nuclear orientation experiment was found to be 0.123(11). This value leads for a target nucleus with a magnetic moment of −1.10 nm and a spin J_t of $\frac{7}{2}$ in a magnetic field of 7.5 T to an average target temperature of 10(1) mK. The fact that this value is much lower than the value

TABLE 11

Results from analysis of the nuclear orientation and of the circular polarization measurements for ^{50}Ti states

E_x	$E_\gamma + E_r$	A_1^{10}	A_0^{11}	A_2^{11}	J
(keV)					
1554	9385	−0.52 (5)	−1.01 (5)	−0.13 (7)	2
2675	8264	0.58 (4)	−0.94 (5)	−0.12 (6)	4
4147	6792	−0.36 (5)	0.38 (5)	−0.06 (11)	4
4172	6767	−0.16 (6)	−0.92 (3)	0.17 (4)	3
4790	6149	−0.4 (4)			(2–5)
4881	6058	−0.43 (5)	0.77 (6)	0.14 (7)	5
5186	5753	0.70 (10)			(3, 4)
5380	5559	0.90 (7)	−0.30 (9)	−0.39 (11)	4
5947	4993	−0.02 (10)	0.33 (12)	−0.37 (14)	(3, 4)
6123	4816	−0.3 (4)	0.9 (4)	0.3 (5)	(3–5)
6302	4637	−0.16 (17)	−0.68 (25)	0.0 (3)	(2–4)
6521	4418	0.58 (22)	0.0 (3)	0.5 (4)	(3, 4)
6711	4229	0.90 (11)	−0.54 (14)	−0.23 (16)	4
6730	4209	0.3 (4)			(2–5)

obtained with the ^{47}Ti sample is caused by the better heat conductivity between sample and target holder.

In table 11 the A-coefficients, obtained from the nuclear orientation and circular polarization experiments, are presented together with the spins or spin restrictions obtained from them. Just as in the ^{47}Ti experiments there are more and better values for A_1^{10} than for A_0^{11} and A_2^{11}.

For the first two excited states at 1554 and 2675 keV the spin assignments of $J = 2$ and 4 [ref. [32])], respectively, were confirmed in the present experiments. In ref. [10]) tentative assignments of $J = 4$ and 2 were made for the states at 4147 and 4172 keV, respectively. In the present work unambiguous assignments could be made of $J = 4$ and $J = 3$, respectively. According to shell-model calculations [33,34]) (see sect. 11) there is a $J = 5$ state near 4.9 MeV, which is confirmed by the present assignment of $J = 5$ to the 4881 keV state. This result is in contradiction with the data from (p, p′) measurements [6,7]), where a spin of $J = 2$ has been derived from the reported momentum transfer of $L = 2$. Two further $J = 4$ assignments were made to the 5380 and 6711 keV states. The former value agrees with the tentative $L = 4$ value, obtained in a (p, p′) measurement [7]). The investigation yielded spin restrictions for the remaining seven states listed in table 11.

From the data of table 11 the average channel spin admixture $\langle \alpha_f \rangle$ can be calculated. For the presented primaries, which have a total strength of 68.4(4)%, a value of −0.32(7) is found for $\langle A_0^{11} \rangle$, leading to $\langle \alpha_f \rangle = 0.38(4)$. Under the assumption that this value is correct for the total primary strength, it leads to values for σ^- and σ^+,

as defined in subsect. 8.1, of 1.04(10) and 0.63(8) b, respectively. The latest compilation [18]) mentions very different values of 0.34 b for σ^- and of 0.08 b for σ^+. This difference cannot be explained by hard-sphere capture nor by contributions of far-distant resonances. In addition to the suggested $J = 4$ bound level also a $J = 3$ negative-energy level is necessary to explain the present σ-values.

8.3. FINAL RESULTS

An attempt was made to determine the spins and parities of the states identified in the spectroscopic part of this work. All the information of refs. [35,36]) was used and from (d, p) reaction data [8]) the l_n values were used to determine parities. From the present work the results listed in tables 10 and 11 were used. Further the assumption of sect. 7 was maintained that primary transitions have pure dipole character. If the lifetime of the state is not known, the secondary transitions were assumed to be of E1, M1 or E2 character. The lifetimes of some ^{48}Ti states are known [11]). Then the RUL's [37]) can be used to determine the character of secondary transitions. The final conclusions are listed in the first and fifth column of table 4 for ^{48}Ti and of table 5 for ^{50}Ti. Altogether six new unambiguous spin and parity determinations were made for ^{48}Ti and five for ^{50}Ti states.

9. Neutron-capture mechanism

The nature of the neutron-capture mechanism was investigated as described in ref. [1]) with the aid of the potential capture formalism [38]). This formalism uses the correlation ρ between the reduced primary γ-ray strength I_γ / E_γ^n and the (d, p) spectroscopic factor, calculated for all levels excited with $l_n = 1$. The optimum correlation, for a variation of the reduction factor n, indicates the nature of the capture mechanism. The data of tables 8 and 9 were used, where a comparison is made between the results of the present work and the (d, p) work. It is shown that most levels excited with $l_n = 1$ are excited by primaries in the present work as well. The total spectroscopic factor for p-states is 4.1(4) for ^{48}Ti and 4.3(4) for ^{50}Ti, while the sum-rule limit is 6.0. In the present investigation thus about $\frac{2}{3}$ of the sum-rule limit is detected in both ^{48}Ti and ^{50}Ti.

In fig. 4a the correlation curves for ^{47}Ti, ^{48}Ti [ref. [1])] and ^{49}Ti target nuclei are drawn. In order to calculate the error at the position of the maximum correlation for each nucleus 1000 data sets were generated by adding to the intensities and spectroscopic factors their respective errors multiplied by a gaussian-distributed random generator (Monte-Carlo process). For each of these data sets the position of the maximum correlation was calculated. In fig. 4b the results are presented as a histogram and the three peaks are fitted with a gaussian-shaped curve, where the width of the curve represents the error at the position of the maximum correlation. The values obtained are $n = 5.4(5)$, 2.31(17) and 1.31(15) for ^{47}Ti, ^{48}Ti and ^{49}Ti,

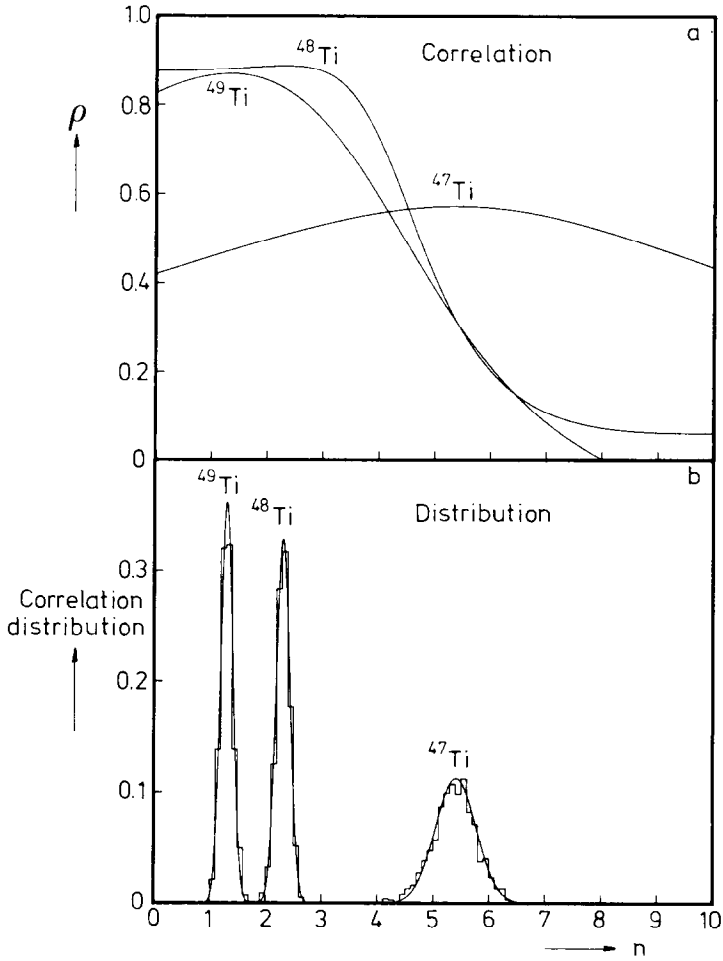

Fig. 4. (a) Correlation between the reduced primary γ-ray strength I_γ/E_γ^n and spectroscopic factors $(2J_f+1)S_{dp}$ versus reduction factor n for p-states. The target nuclei are indicated. (b) Distribution of the position of the maximum of the correlation curve (see upper part) for redistributed data sets (see text). The resulting peaks are fitted with gaussian-shaped curves. The distributions are normalized to unity.

respectively. These very different values suggest different thermal neutron-capture mechanisms.

Lane and Lynn [38]) have proposed a formalism of potential capture, in which hard-sphere and resonance contributions interfere coherently. In evaluating the expression for the partial cross sections one finds that the hard-sphere contribution has an optimum correlation near $n = 1$ and the resonance part near $n = 2$. Calculations show that for ^{48}Ti the resonance part is predominant and that for ^{49}Ti the two terms give about equal contributions. The cross section for transitions to p-states is 7.71(25) b for ^{48}Ti and 1.38(11) b for ^{49}Ti. Although the potential capture

estimate [38]) agrees well for ^{48}Ti, 8.1(8) b, it estimates the value for ^{49}Ti, 0.37(4) b, low by a factor of 4. Two possible explanations for this deviation are either a wrong value for the coherent scattering length [18]) or a non-negligible statistical contribution to the cross section. The behaviour of the ^{47}Ti nucleus does not fit at all in the framework of potential capture. The fact that the optimum correlation, 0.56(15), is significantly different from zero indicates doorway capture.

10. Level density

As described in ref. [1]) the ^{48}Ti and ^{50}Ti nuclear level densities were compared with the theoretical approach given by Bethe [39]), who treated the nucleus as a system of noninteracting fermions distributed over equally spaced single-particle levels. In the present analysis it was assumed that up to $E_x = 5.0$ MeV all ^{48}Ti states with $J = (1\text{–}4)$ and all ^{50}Ti states with $J = (2\text{–}5)$ are excited by primaries. The level density at the capture state was derived from ref. [18]).

In fig. 5 where the fits are presented of the cumulative number of levels it is clearly shown that above $E_x = 5.0$ MeV we start to miss levels in the indicated spin range, whereas at lower energies there is good agreement. The model is described by two parameters: the Fermi energy E_0 and the single-particle level density parameter a. For E_0 we find values of 0.87(9) MeV for ^{48}Ti and 1.69(18) MeV for ^{50}Ti. The a-values for these nuclei are 5.27(10) MeV^{-1} and 5.39(13) MeV^{-1}, respectively. These values are in good agreement with liquid drop model calculations [40]), which yield values of 5.40 and 5.61 MeV^{-1}, respectively.

11. Shell model

Recently a computer code became available which enabled shell-model calculations for ^{48}Ti and ^{50}Ti. A semi-empirical interaction was used, which has been optimized to reproduce excitation energies in $A = 52\text{–}60$ nuclei [41]). The configuration space is represented by f^n and $f^{n-1}r^1$, where f denotes the $1f_{7/2}$ orbit and r stands for the other fp orbits. The number of active particles (8 in ^{48}Ti and 10 in ^{50}Ti) is given by n. An inert ^{40}Ca core was used. The lowest four eigenvalues for each possible spin were calculated together with the M1 and E2 γ-ray widths. The effective charges used for proton and neutron are 1.5 e and 0.5 e, respectively. The widths were converted into branching ratios and lifetimes.

In fig. 6 the results for ^{48}Ti are compared with experimental data. Although the calculated excitation energies are on the average lower than the experimental values, there is a good agreement for the lowest nine states. The 0_2^+ state could not be represented satisfactorily. A calculation in which the configuration space was extended with $f^{n-2}r^2$ shows that the level at $E_x = 3696$ keV corresponds to the 0_3^+ state and that the 0_2^+ state consists almost entirely of 2p2h components.

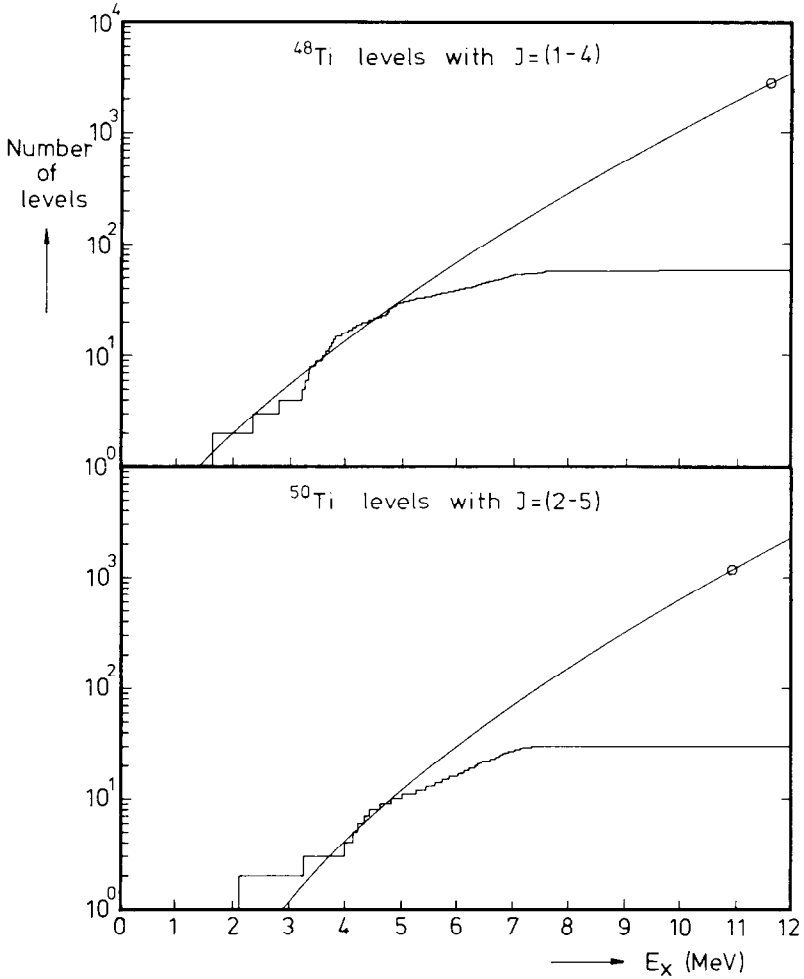

Fig. 5. The cumulative number of levels excited by (n, γ) primaries as a function of excitation energy, and the resonance level density for ^{48}Ti (upper part) and for ^{50}Ti (lower part). In both cases the levels below $E_x = 5.0$ MeV are included in the fit. For the theoretical curves, see text.

The calculations suggest that the 3240 keV state has a spin of $J = 4$ and that there is a $J = 1$ state near 3700 keV. For the latter there are two possible candidates, the $J^\pi = (1, 2^+)$ state at $E_x = 3699$ keV and the $J^\pi = (1, 2)^+$ state at $E_x = 3739$ keV. In further calculations we have assumed that the 3739 keV state has $J = 1$, but the results do not change significantly if the other choice is made. From table 12, where experimental and theoretical branching ratios and lifetimes are compared, it may be concluded that in the calculations M1 strength is overestimated and E2 strength underestimated. This is also reflected by the lifetimes.

In ^{50}Ti there is also a good agreement between the theoretical and experimental values for the excitation energies of the lowest eight levels, as is shown in fig. 6. If

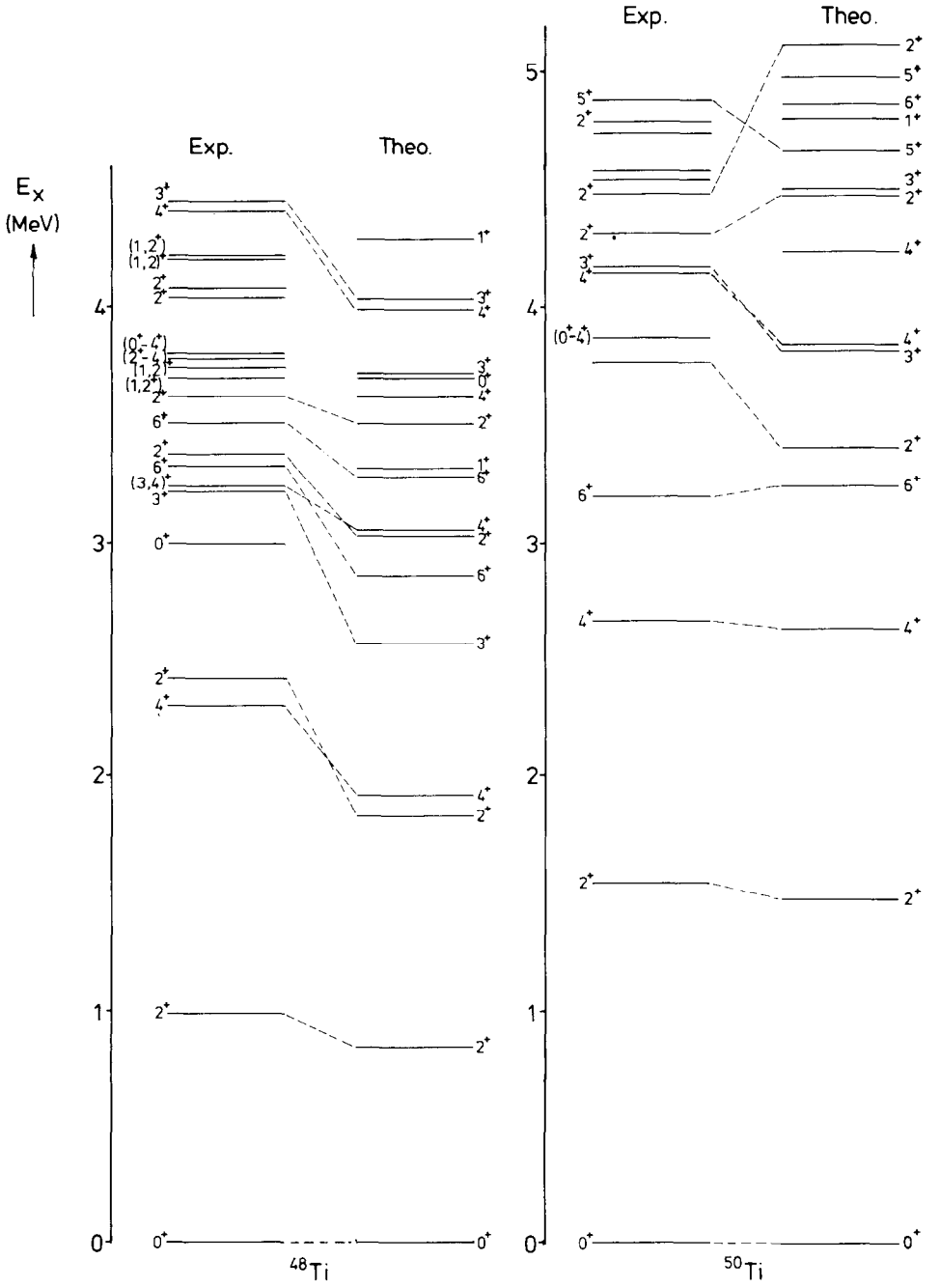

Fig. 6. Comparison between calculated and measured excitation energies of low-lying states in ^{48}Ti (left-hand part) and ^{50}Ti (right-hand part).

TABLE 12

Results from shell-model calculations compared to experimental data for ^{48}Ti

E_{xi} (keV)	J^π	E_{xf} (keV)	Branching (%)		τ_m (fs)	
			exp.	theo.	exp.	theo.
984	2^+	0	100	100	6060	25×10^3
2296	4^+	984	100	100	1400	4100
2421	2^+	0	5	1	60	17
		984	95	99		
2997	0^+	984	100		125	
3224	3^+	984	73	87	78	6
		2296	23	9		
		2421	3	4		
3240	4^+	2296	100	100	70	15
3333	6^+	2296	100	100	>5000	17×10^3
3371	2^+	0	16	1	<40	3
		984	84	99		
3617	2^+	0	1	<1	55	4
		984	92	88		
		2421	7	12		
3739	1^+	0	62	73	16	2
		984	38	13		
		2421	<20	14		
4388	4^+	984	54	<1	50	5
		2296	46	81		
		2421	<5	19		
4457	3^+	984	22	68	70	5
		2296	39	2		
		2421	33	11		
		3224	1	17		
		3371	2	2		
		3617	3	<1		

the $L=0$ assignment from the $^{48}Ti(t, p)^{50}Ti$ reaction [10]) is accepted for the level at $E_x = 3863$ keV, then just as in ^{48}Ti the 1p1h calculations fail to represent the 0_2^+ state, which also appears to have almost exclusively a 2p2h structure. A spin of $J=2$ is suggested for the level at $E_x = 3763(8)$ keV, which is not excited in (n, γ). If we examine the sequence of theoretical $J=2$ states it seems that the distance between the levels is too large.

If the target ground-state wave function is known as well as the final-state wave functions, the (d, p) spectroscopic factor can be calculated. We only know the wave function of the ^{49}Ti ground state, and not that of ^{47}Ti, so only for ^{50}Ti the $l_n=1$ part of the spectroscopic factors was calculated, which is compared in table 13 together with the branching ratios to the experimental results. For the 4310 and 4881 keV states the theoretical and experimental branching ratios appear to deviate. Also the spectroscopic factor of the 4310 keV level is overestimated by one

TABLE 13

Results from shell-model calculations compared to experimental data for ^{50}Ti

E_{xi} (keV)	J^π	E_{xf} (keV)	Branching (%)		$(2J_f+1)S_{dp}$ [a]	
			exp.	theo.	exp.	theo.
1554	2^+	0	100	100	0.08	0.046
2675	4^+	1554	100	100	0.04	0.026
3199	6^+	2675	100	100		
3763	2^+	0		66		0.004
		1554		34		
3863	0^+	1554	100			
4147	4^+	2675	100	100	0.74	0.779
4172	3^+	1554	68	91	0.93	0.618
		2675	32	8		
		3763	<5	1		
4310	2^+	0	16	<1	0.02	0.243
		1554	84	100		
4487	2^+	0	14	3		0.138
		1554	86	97		
4881	5^+	2675	90	10	0.81	0.637
		3199	8	77		
		4147	2	13		

[a]) The $l_n = 1$ parts are being compared.

order of magnitude. For the other levels the theoretical spectroscopic factors are small by only a factor of 1.2. There is also a good correlation of 0.92 between the two sets.

12. Conclusions

Accurate excitation energies are determined for 57 states in ^{48}Ti and for 31 states in ^{50}Ti. Absolute intensities were determined by postulating the total strength to the ground state as 100%. Under this assumption a large part of the primary strength is missing, 26.2(4)% in ^{48}Ti and 16.8(6)% in ^{50}Ti, just as in other even–even nuclei. The ^{47}Ti and ^{49}Ti thermal neutron cross sections are determined as 1.48(9) and 1.67(12) b, respectively. The value of 11 626.66(4) keV found for the ^{48}Ti neutron binding energy is in agreement with a previous measurement. The difference of five standard deviations between the present value for the ^{50}Ti neutron binding energy of 10 939.20(4) keV and the previous value of 10 939.7(1) keV is presumably caused by the small number of cascades used in the previous work. It is shown that for ^{47}Ti the neutron-capture process proceeds through a doorway state, whereas for ^{49}Ti the potential capture formalism is valid. The density of levels, excited by primary dipole transitions, and the level density at the capture state are for both nuclei explained satisfactorily by the Fermi gas model.

By combining the results of a nuclear orientation measurement and of a circular polarization measurement with the ^{47}Ti target the spin of one ^{48}Ti state is determined, the previously known spins of three states are confirmed and the spins of 15 states could be restricted. A further analysis, in which all available information, also from previous work, is included, yields unambiguous spin and parity assignments for another six states.

The spins of five states in ^{50}Ti could be unambiguously assigned from the analysis of the two measurements, the previously known spins of two excited states were confirmed and restrictions could be made for the spins of seven other states. The further analysis of the decay scheme yielded another five unambiguous spin and parity determinations for ^{50}Ti states.

The results from 1p1h shell-model calculations show good agreement with the experimentally determined low-lying states in both nuclei. Both 0_2^+ states are reproduced only if also 2p2h excitations are taken into account. The E2 and M1 strengths are under- and over-estimated, respectively.

We wish to thank Mr. P. Hokkeling of the Philips Natuurkundig Laboratorium in Eindhoven for the support he gave in the metallurgical and chemical aspects of the target reduction.

References

1) J.F.A.G. Ruyl and P.M. Endt, Nucl. Phys. **A407** (1983) 60
2) P. Fettweis and M. Saidane, Nucl. Phys. **A139** (1969) 113
3) J. Tenenbaum, R. Moreh, Y. Wand and G. Ben-David, Phys. Rev. **C5** (1971) 663
4) J. Tenenbaum, R. Moreh, Y. Wand and G. Ben-David, Phys. Rev. **187** (1969) 1403
5) A. Jamshidi and W.P. Alford, Phys. Rev. **C8** (1973) 1796
6) H.F. Lutz, W. Bartolini, T.H. Curtis and G.M. Klody, Phys. Rev. **187** (1969) 1479
7) B.M. Preedom, C.R. Gruhn, T.Y.T. Kuo and C.J. Maggiore, Phys. Rev. **C2** (1970) 166
8) P. Wilhjelm *et al.*, Phys. Rev. **166** (1968) 1121
9) H.W. Baer *et al.*, Ann. of Phys. **76** (1973) 437
10) S. Hinds and R. Middleton, Nucl. Phys. **A92** (1967) 422
11) F. Glatz *et al.*, Z. Phys. **A293** (1979) 57
12) T.T. Bardin, J.A. Becker and T.R. Fisher, Phys. Rev. **C7** (1973) 190
13) J.G. Pronko *et al.*, Phys. Rev. **C10** (1974) 1345
14) C. van der Leun and C. Alderliesten, Nucl. Phys. **A380** (1982) 261
15) R.C. Greenwood and R.E. Chrien, Nucl. Instr. **175** (1980) 515
16) R.G. Helmer, P.H.M. van Assche and C. van der Leun, Atom. Nucl. Data Tables **24** (1979) 39
17) Handbook of chemistry and physics, 56th ed. (CRC Press, 1975) B338
18) S.F. Mughabghab, M. Divadeenam and N.E. Holden, Neutron cross sections, vol. 1, part A (Academic, New York, 1981)
19) E.G. Kessler, R.D. Deslattes, A. Henins and W.C. Sauder, Phys. Rev. Lett. **40** (1978) 171
20) J.K. Dickens, Nucl. Sci. Eng. **54** (1974) 191
21) C.F. Monahan, J.G. Main, F.M. Nicholas, M.F. Thomas and P.J. Twin, Nucl. Phys. **A130** (1969) 209
22) J.H. Bjerregaard, P.F. Dahl, O. Hansen and G. Sidenius, Nucl. Phys. **51** (1964) 641
23) S.V. Jackson, E.A. Henry and R.A. Meyer, J. Inorg. Nucl. Chem. **38** (1976) 1099
24) M.A. Islam, T.J. Kennett, S.A. Kerr and W.V. Prestwich, Can. J. Phys. **58** (1980) 168
25) D.H. White and R.E. Birkett, Phys. Rev. **C5** (1972) 513

26) U. Fanger *et al.*, Nucl. Phys. **A146** (1970) 549
27) W. Freundlich and M. Bichara, Compt. Rend. **238** (1954) 1324
28) J.J. Bosman and H. Postma, Nucl. Instr. **148** (1978) 331
29) F. Stecher-Rasmussen, K. Abrahams and J. Kopecky, Nucl. Phys. **A181** (1972) 225
30) A.N. James, P.J. Twin and P.A. Butler, Nucl. Instr. **115** (1974) 105
31) P.P.J. Delhey, A. Girgin, K. Abrahams, H. Postma and W.J. Huiskamp, Nucl. Phys. **A341** (1980) 21
32) G. Chilosi, P. Cuzzocrea, G.B. Vingiani, R.A. Ricci and H. Moringa, Nuovo Cim. **27** (1963) 86
33) I.P. Johnstone, Phys. Rev. **C17** (1978) 1428
34) B. Haas *et al.*, Phys. Rev. Lett. **40** (1978) 1313
35) Nucl. Data Sheets **23** (1978) 36
36) Nucl. Data Sheets **19** (1976) 305
37) P.M. Endt, Atom. Nucl. Data Tables **23** (1979) 3
38) A.M. Lane and J.E. Lynn, Nucl. Phys. **17** (1960) 563, 586
39) H.A. Bethe, Phys. Rev. **50** (1936) 332
40) S.K. Kataria and V.S. Ramamurthy, Nucl. Phys. **A349** (1980) 10
41) R.B.M. Mooy, P.W.M. Glaudemans and A.G.M. van Hees, Phys. Lett. **104B** (1981) 251